พฤติกรรมการยึดเหนี่ยวระหว่างคอนกรีตเสริมเหล็กหลังถูกเพลิงไหม้
และวัสดุโพลิเมอร์เสริมเส้นใยคาร์บอน

นางสาว พรเพ็ญ ลิมปนิลชาติ

วิทยานิพนธ์นี้เป็นส่วนหนึ่งของการศึกษาตามหลักสูตรปริญญาวิศวกรรมศาสตรมหาบัณฑิต
สาขาวิชาวิศวกรรมโยธา ภาควิชาวิศวกรรมโยธา
คณะวิศวกรรมศาสตร์ จุฬาลงกรณ์มหาวิทยาลัย
ปีการศึกษา 2555

BONDING BEHAVIOR BETWEEN REINFORCED CONCRETE AFTER FIRE AND CARBON FIBER REINFORCED POLYMER

Miss Pornpen Limpaninlachat

A Thesis Submitted in Partial Fulfillment of the Requirements
for the Degree of Master of Engineering Program in Civil Engineering
Department of Civil Engineering
Faculty of Engineering
Chulalongkorn University
Academic Year 2012

Thesis Title	BONDING BEHAVIOR BETWEEN REINFORCED CONCRETE AFTER FIRE AND CARBON FIBER REINFORCED POLYMER
By	Miss Pornpen Limpaninlachat
Field of Study	Civil Engineering
Thesis Advisor	Assistant Professor Withit Pansuk, Ph.D.

Accepted by the Faculty of Engineering, Chulalongkorn University in Partial Fulfillment of the Requirements for the Master's Degree

………………………………………… Dean of the Faculty of Engineering

(Associate Professor Boonsom Lerdhirunwong, Dr.Ing.)

THESIS COMMITTEE

………………………………………… Chairman

(Professor Thaksin Thepchatri, Ph.D.)

…………………………………………Thesis Advisor

(Assistant Professor Withit Pansuk, Ph.D.)

………………………………………… Examiner

(Associate Professor Thanyawat Pothisir, Ph.D.)

…………………………………………External Examiner

(Krit Laosiriphong, Ph.D.)

พรเพ็ญ ลิมปนิลชาติ : พฤติกรรมการยึดเหนี่ยวระหว่างคอนกรีตเสริมเหล็กหลังถูกเพลิงไหม้และวัสดุโพลิเมอร์เสริมเส้นใยคาร์บอน. (BONDING BEHAVIOR BETWEEN REINFORCED CONCRETE AFTER FIRE AND CARBON FIBER REINFORCED POLYMER) อ. ที่ปรึกษาวิทยานิพนธ์หลัก: ผศ.ดร. วิทิต ปานสุข , 71 หน้า.

จากเหตุการณ์ที่ผ่านมามีอุบัติเหตุเพลิงไหม้เกิดขึ้นเป็นจำนวนมากในหลายๆประเทศทั่วโลกรวมทั้งในประเทศไทย อุบัติเหตุเหล่านั้นได้สร้างความเสียหายอย่างรุนแรงต่อโครงสร้าง ส่งผลให้โครงสร้างมีประสิทธิภาพการใช้งานลดน้อยลง ตัวอย่างผลกระทบจากเพลิงไหม้ที่สร้างความเสียหายให้แก่โครงสร้างคอนกรีตเสริมเหล็ก คือ กำลังของโครงสร้างลดลง, สูญเสียแรงยึดเหนี่ยวระหว่างเหล็กเสริมและคอนกรีต และเกิดการแตกร้าวที่ผิวของคอนกรีต ในปัจจุบันการเสริมกำลังของโครสร้างสามารถทำได้หลายวิธี หนึ่งในวิธีที่ได้รับความนิยมคือการเสริมกำลังโครงสร้างด้วยวัสดุโพลิเมอร์เสริมเส้นใย เนื่องจากเป็นวัสดุที่มีอัตราส่วนกำลังต่อน้ำหนักสูง มีความสามารถทนทานต่อการกัดกร่อนสูง และเป็นวัสดุที่สะดวกต่อการนำมาใช้หน้างาน เป็นต้น ดังนั้นงานวิจัยนี้จึงทำการศึกษาผลกระทบจากเพลิงไหม้ที่มีผลต่อการยึดเหนี่ยวระหว่างโครงสร้างที่เสียหายและวัสดุโพลิเมอร์เสริมเส้นใยคาร์บอนเพื่อทำการสร้างแบบจำลอง interfacial stress-slip โดยในการศึกษาครั้งนี้ได้ทำการจำลองอุณหภูมิของเพลิงไหม้ตามมาตรฐานกราฟอุณหภูมิเปลวไฟ-เวลา ASTM E119 และกำหนดให้ อุณหภูมิของไฟ (0, 45, 90 นาที), ความยาวของวัสดุโพลิเมอร์เสริมเส้นใย (15, 20, 30 เซนติเมตร) และ ระยะหุ้มเหล็กเสริม (1, 2, 3 เซนติเมตร) เป็นตัวแปรในการทดลอง หลังจากทำการทดสอบตัวอย่างด้วยวิธี Modified pull out test จะสามารถสร้างกราฟการกระจายความเครียด ซึ่งเป็นขั้นตอนพื้นฐานของการสร้างแบบจำลอง interfacial stress-slip ระหว่างคอนกรีตที่เสียหายและวัสดุโพลิเมอร์เสริมเส้นใย

ภาควิชา วิศวกรรมโยธา ลายมือชื่อนิสิต____________________
สาขาวิชา วิศวกรรมโยธา ลายมือชื่อ อ.ที่ปรึกษาวิทยานิพนธ์หลัก __________
ปีการศึกษา 2555

5370560221 : MAJOR CIVIL ENGINEERING
KEYWORDS : BOND TEST / INTERFACIAL FRACTURE ENERGY / FIRE EXPOSURE / CONCRETE COVERING / FRP

PORNPEN LIMPANINLACHAT : BONDING BEHAVIOR BETWEEN REINFORCED CONCRETE AFTER FIRE AND CARBON FIBER REINFORCED POLYMER. ADVISOR : ASSIST. PROF. WITHIT PANSUK, Ph.D., 71 pp.

Nowadays, the fire accidents of building frequently occur in many countries including in Thailand and cause severe damages to structures. Those critical incidents can diminish the concrete strength, reduce bond strength between concrete and steel reinforcement and spalling occurs on concrete surface. Consequently, the structural repair by strengthening with Fiber Reinforced Polymer (FRP) is one of the popular solutions owing to high strength to weight ratio, high corrosion resistance and conveniently in situ at construction site. This research focused on the effects of interfacial bond stress in order to investigate the bonding behavior of concrete exposed to fire according to standard temperature-time curve of ASTM E119. To accomplish this, the strain distribution was obtained from the modified pull out test and three parameters were varied; concrete covering, bond length and exposed time to fire. Concrete specimens varied with concrete covering 1, 2 and 3 cm were burnt with different time exposures (0, 45 and 90 minutes) and attached with Carbon Fiber Reinforced Polymer (CFRP) through epoxy. The attached CFRP also had various bond lengths; 15, 20 and 30 cm. Finally, the important parameters for bonding behavior were shown in term of interfacial fracture energy from experimental data.

Department : Civil Engineering .... Student's Signature ....
Field of Study : Civil Engineering .... Advisor's Signature ....
Academic Year : 2012 ....

ACKNOWLEDGEMENTS

This thesis succeeded by many advocators. Firstly, I would like to express my deepest appreciation and sincere gratitude to my advisor, Assistant Professor Dr. Withit Pansuk. Thank you for his valuable guidance, excellent counseling, problem solving, continuous support, throughout my master study. Secondly, I would like to express my great appreciation to my thesis committees for their valuable and constructive suggestions. Thirdly, I would like to express my thankfulness to Associate Professor Dr. Phoonsak Pheinsusom and academic staffs in department of civil engineering for their helpfulness in successful coordination to JASSO scholarship. Next, I am particularly grateful to Professor Junichiro Niwa and Assistant professor Koji Matsumoto from Tokyo Institute of technology for their useful recommendations on this study. I also would like to offer my special thanks to Associate professor Boonchai Stitmannaithum for his class about concrete technology that inspired me to create my valuable study in the concrete field. I would like to thanks Chulalongkorn University and Japan Student Services Organization for their financial supports and Sika (Thailand) Limited for the material supporting that helping me to complete my master study. Moreover, I would like to thank all lecturers and staff in Department of Civil Engineering, Chulalongkorn University for their greatful help that made this study flow effortlessly, including find out the place that were used to collect data. My grateful thanks are also extended to Mr. Siwarak Unsiwilai, Mr. Anuwat Attachaiwuth, Mr. Totsawat Daungwilailuk and other structural members for their helpfulness in collecting data.

Finally, I wish to express infinite gratitude and my deepest to my beloved parents and everybody in my family, and my relatives for their love, assistances, warmest support, excellent suggestion and the best understanding to inspired me for complete this study.

CONTENTS

Page

LIST OF FIGURES

Page

Page

Page

LIST OF TABLES

Page

CHAPTER I
INTRODUCTION

1.1 General

There are many deterioration mechanisms affecting reinforced concrete (RC) structures. Fire accidents on building are the one that cause severe damages to structures and frequently occur all over the world. Those critical actions can diminish the concrete strength, reduce bond strength between concrete and steel reinforcement, and create damages at concrete surface. Thus, those reinforced concrete structures after fire cannot be effectively used as it was. Nowadays, new technologies and materials for strengthening purpose have been invented to repair or improve the performance of structures. Consequently, the structural strengthened using Fiber Reinforced Polymer (FRP) is one of the popular solutions because of its high strength-to-weight ratio, high corrosion resistance, and high energy absorption. Due to the mentioned properties, they lead to site handling, durable performance, reducing labor cost and less interruption of existing service. FRP can be attached with RC beams and RC columns in various configurations in order to increase stiffness and strength of members. However, from previous researches, the way to use FRP efficiently depends on bond behavior which is important to a whole behavior of member. Accordingly, the assumption in this research is that the effects of fire may change bond behavior between FRP and concrete after fire.

This research focuses on the effects of fire on interfacial bond behavior in order to model the interfacial stress-slip relationship of FRP to concrete after fire exposure condition, which is controlled by standard temperature-time curve of ASTM E119 [17]. To accomplish this, the strain distribution on FRP attached to damaged concrete surface will be obtained from the modified pull-out test and three parameters will be varied; concrete covering, exposed time to fire and bond length. Concrete specimens with dimension of 10x10x50 cm and varied covering between 1 to 3 cm will be burnt with different time exposures (0, 45 and 90 minutes) and bonded with Carbon Fiber Reinforced Plastic (CFRP) by epoxy material before the pull-out test. The interfacial stress-slip relationship (τ-S model) of reinforced concrete after fire exposures and CFRP which includes the effects of concrete covering, exposed time to fire and bond length can be derived from the results of pull-out test by modifying the existing models for RC members without fire exposure. Finally, the proposed model will be conducted to show the effect of fire on bonding behavior of reinforced concrete after fired and CFRP plate.

1.2 Research Objectives

1. To study the effects of fire exposure time, concrete covering and bond length on interfacial bond behavior between reinforced concrete after fire exposures and Carbon Fiber Reinforced Plastic (CFRP).
2. To model the interfacial bond stress-slip model (τ-S model) of reinforced concrete after fire exposures attached to Carbon Fiber Reinforced Plastic (CFRP).

1.3 Scopes of Research

1. The installation and testing of fire exposure is operated under ASTM E119 standard [17].
2. The strengthening design of Carbon Fiber Reinforced Plastic (CFRP) is operated under ACI-440.2R-02 specification [2].
3. The installation of CFRP on concrete surface is operated under the standard of the department of public works and town & country planning (DPT 1508-51 standard).
4. In this study, only the plate-end debonding failures are considered.
5. The interfacial bond behavior between reinforced concrete after fire exposures and Carbon Fiber Reinforced Plastic (CFRP) are considered under the effects of fire exposure time, concrete covering and bond length.
6. The load test is operated under room temperature.

CHAPTER II
LITERATURE REVIEW

2.1 Introduction of FRP [1]

Fiber Reinforced Polymer (FRP) was invented since 1993 the Swiss Federal Laboratory for Materials Testing and Research (EMPA). Due to numerous researches about FRP and their advantages as high strength-to-weight ratio, high corrosion resistance, convenience for using in site construction and reducing labor cost, FRP becomes a popular material for strengthening deficient RC structures worldwide. In general, there are three types of FRP; sheet, plate and rod which are applied in various shapes depending on structure characteristics such as in strengthening Reinforced Concrete (RC) column; FRP is installed by external wrapping. Not only in RC structures, FRP composites have been used in other areas also for instance the steel structures, the aerospace industry, the automotive industry and in the marine structures.

FRP composite is a material made of a resin matrix reinforced with continuous fibers. The common fibers are fiberglass, carbon fibers, aramid fibers as shown in Figure 1, whilst the polymer is usually an epoxy resins, vinylester resins and polyester resins depending on the fibers used. The typical mechanical properties of each FRP are referred from ACI 440.2R-02 [2] as shown in Table 1.

Figure1 Examples of Fibers

Table 1 Typical mechanical properties of Glass Fiber Reinforced Plastic (GFRP), Carbon Fiber Reinforced Plastic (CFRP) and Aramid Fiber Reinforced Plastic (AFRP) with fiber volumes of 40 to 60 % [2]

Unidirectional advanced composite materials	Density (kg/m^3)	Longitudinal tensile modulus (GPa)	Tensile Strength (MPa)
Glass fiber/polyester GFRP laminate	1200-2100	20-40	520-1400
Carbon/epoxy CFRP laminate	1500-1600	100-140	1020-2080
Aramid/epoxy AFRP laminate	1200-1500	48-68	700-1720

2.2 Bond Strength Models

From several bond strength models proposed by former researches can be classified into three categories and developed for both steel plates and FRP plates as empirical models, fracture mechanics models and design proposals.

2.2.1 Empirical Models are derived based on the regression of test directly as shown in Tables 2.

Table 2 Review of the empirical models

Researcher	Model	Equation	Remark
1. Hiroyuki and Wu [3] tested the specimens by double shear on RC member which strengthened with	$\tau_u = 5.88L^{-0.669}$, MPa	2.1	• τ_u = average bond shear stress at failure • L = bond length (cm)

Researcher	Model	Equation	Remark
Carbon Fiber Sheet (CFS).			
2. Tanaka [4]	$\tau_u = 6.13 - \ln L$, MPa	2.2	• L = bond length (mm.)
3. Maeda et al. [5] developed the stronger model by considered the effect of effective bond length	$\tau_u = 110.2 \times 10^{-6} E_p t_p$, MPa $L_e = e^{6.13-0.580 ln E_p t_p}$,mm	2.3a 2.3b	• E_p = elastic modulus of the bond plate (MPa) • t_p = thickness of the bond plate (mm) • For 2.3b, noted that $E_p t_p$ is in GPa-mm. And this model certainly valid if $L < L_e$

From equations 2.1 and 2.2, the ultimate bond strength of the joint P_U is referred by τ_U multiplied by width of plate b_p and length L of bond area. However in equation 2.3, the determination of the ultimate bond strength of the joint P_U is presented by τ_U multiplied by width of plate b_p and effective bond length L_e

2.2.2 Fracture-mechanics-based Models are directly represented in bond strength, P_u as shown in Tables 3.

Table 3 Review of the fracture-mechanics-based models

Researcher	Model	Equation
1. Holzenkämpfer [6] investigated the relationship to find out the bonding strength between steel and concrete by using	$P_u = \begin{cases} 0.78 b_p \sqrt{2 G_f E_p t_p} & , \text{if } L \geq L_e \\ 0.78 b_p \sqrt{2 G_f E_p t_p} \dfrac{L}{L_e}\left(2 - \dfrac{L}{L_e}\right) & , \text{if } L < L_e \end{cases}$ $L_e = \sqrt{\dfrac{E_p t_p}{4 f_{ctm}}}$, mm $G_f = C_f k_p^2 f_{ctm}$, N mm/mm^2	2.4a 2.4b 2.4c

<table>
<tr><th>Researcher</th><th>Model</th><th>Equation</th></tr>
<tr><td>nonlinear fracture mechanics (NLFM)</td><td>$\mathrm{k_p} = \sqrt{1.125\dfrac{2-b_p/b_c}{1+b_p/400}}$</td><td></td></tr>
<tr><td colspan="3">Remark E_pt_p is in MPa-mm, P_U is in N, f_{ctm} is an average surface tensile strength of the concrete from the pull-off (MPa) and c_f is a constant defined in a linear regression analysis from the double shear test or similar tests. Moreover the parameter k_p is a geometrical factor related to the width of bonded plate b_p and concrete member b_c (mm)</td></tr>
<tr><td>2. <u>Täljsten</u> [7] also developed the model by NLFM</td><td>$\mathrm{P_u} = \sqrt{\dfrac{2E_pt_pG_f}{1+\propto_T}}b_p$
$\propto_\mathrm{T} = \dfrac{E_pt_p}{E_ct_c}$</td><td>2.5a
2.5b</td></tr>
<tr><td colspan="3">Remark
• E_c is the elastic modulus of concrete member
• t_c is the thickness of concrete member
• In this model, the determination of G_f is not clearify.</td></tr>
<tr><td>3. <u>Yuan and Wu</u> [8]
1) Studied bond FRP and concrete by using linear elastic fracture mechanics (LEFM)</td><td>$\mathrm{P_u} = \sqrt{\dfrac{2E_pt_pG_f}{1+\propto_Y}}b_p$
$\propto_\mathrm{Y} = \dfrac{b_pE_pt_p}{b_cE_ct_c}$</td><td>2.6a
2.6b</td></tr>
</table>

Researcher	Model	Equation
2) Yuan et al. [9] also used nonlinear fracture mechanics (NLFM) and obtained fives shear stress-slip relationship (Figure 2). The closest to reality one is as shown in Figure 2d which is derived to be the model.	$\mathrm{P_u} = \frac{\boldsymbol{\tau_f b_p}}{\boldsymbol{\lambda_2}}\frac{\boldsymbol{\delta_f}}{\boldsymbol{\delta_f-\delta_1}}\mathbf{sin}(\boldsymbol{\lambda_2 a})$ *Which a is solved by* $\tanh[\lambda_1(\mathrm{L}-\mathrm{a})] = \frac{\lambda_2}{\lambda_1}\tan(\lambda_2 a)$ $\lambda_1^2 = \frac{\tau_f}{\boldsymbol{\delta_1} E_p t_p}(1+\alpha_Y)$ $\lambda_2^2 = \frac{\tau_f}{(\boldsymbol{\delta_f}-\boldsymbol{\delta_1})E_p t_p}(1+\alpha_Y)$ *Furthermore, the L_e also given as follow* $\mathrm{L_e} = a_0 + \frac{1}{2\lambda_1}\ln\frac{\lambda_1+\lambda_2\tan(\lambda_2 a_0)}{\lambda_1-\lambda_2\tan(\lambda_2 a_0)}$ $a_0 = \frac{1}{\lambda_2}\sin^{-1}\left(0.97\sqrt{\frac{\boldsymbol{\delta_f}-\boldsymbol{\delta_1}}{\boldsymbol{\delta_f}}}\right)$	2.7a 2.7b 2.7c 2.7d 2.7e 2.7f
4. <u>Neubauer and Rostásy</u> [10] tested the sets of CFRP to concrete joints by double shear tests	*From the shear-slip model Figure2d and the fracture energy can represent the G_f as* $\mathrm{G_f} = C_f f_{ctm}$ *Instead of C_f with 0.204 mm. and modified the formula 2.4a into* $\mathrm{P_u} = \begin{cases} 0.64\mathrm{k_p b_p}\sqrt{E_p t_p f_{ctm}} & ,\mathrm{if\ L \geq L_e} \\ 0.64\mathrm{k_p b_p}\sqrt{E_p t_p f_{ctm}}\frac{\mathrm{L}}{\mathrm{L_e}}\left(2-\frac{\mathrm{L}}{\mathrm{L_e}}\right) & ,\mathrm{if\ L < L_e} \end{cases}$ $\mathrm{L_e} = \sqrt{\frac{E_p t_p}{2 f_{ctm}}}$	2.8 2.9a 2.9b

Researcher	Model	Equation
Remark • Consequently, Equation 2.9a and 2.9b can use for both steel and FRP plates. Units of all parameter in equation 2.9 can be used the same as equation 2.4.		

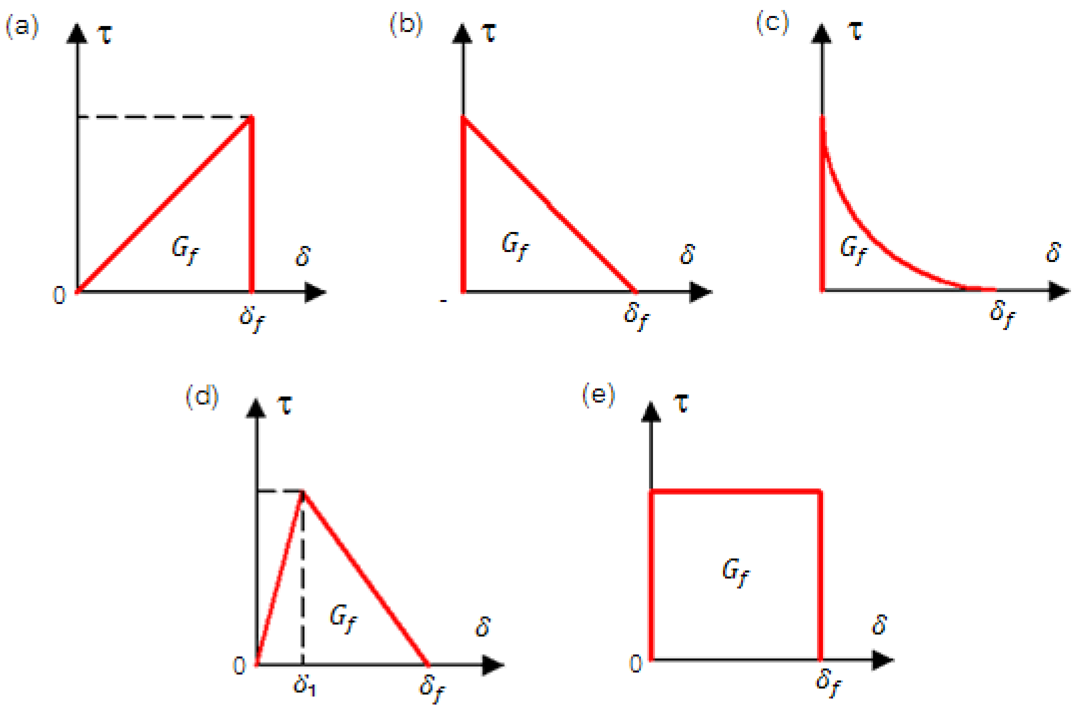

Figure 2 Shear-slip models for FRP bonded to concretes

2.2.3 **Design Proposals Models** are as shown in Table 4.

Table 4 Review of the design proposals models

Researcher	Models	Equation	Remark
1. Van Gemert [11] suggested the design model which assumed from a triangle shear stress	$P_u = 0.5\, b_p L f_{ctm}$, MPa	2.10	• From this design proposal, implies that no matter how much load P increases, plate can be carried out via adequately long

distribution (stress is linearly diminishing from the loaded end to free end)			bonded joint. So this equation is misleading to the concept of FRP that is even though the bond lengths are extended, the strength can't increase.
2.Chaallal at al. [12] assumed that the average stress (τ_u) is a half of the maximum shear stress ($\boldsymbol{\tau_{max}^{debonding}}$),which not more than the Mohr-Coulomb strength equation from Varastehpour and Hamelin [1]	$\tau_u = \frac{\tau_{max}^{debonding}}{2}$, MPa $\tau_u = \dfrac{2.7}{1 + k_1 \tan 33°}$ $k_1 = t_p \sqrt[4]{\dfrac{K_n}{4E_pI_p}}$ $K_n = E_a \dfrac{b_a}{t_a}$	2.11a 2.11b 2.11c	• E_a = Modulus of elasticity of the adhesive • b_a = Width of the adhesive • t_a = Thickness of the adhesive • I_p = Second moment of area of the FRP plate • Disadvantage is that the model does not consider the concrete strength and effective bond length.
3. Khalifa et al. [13] proposed model by adding the effect of concrete strength into Maeda et al. [5]	$\tau_u = \frac{110.2}{10^6}\left(\frac{f_c'}{42}\right)^{\frac{2}{3}} E_p t_p$,MPa	2.12	• $E_p t_p$ is in MPa-mm. • Effective bond length, L_e, can calculate from equation 2.3b.

2.3 Derivation of Bond-Slip Models

From previous study, bond-slip models are developed from various methods. However, three derivations that were considered as a primary model in this study are described as following.

2.3.1 Derivation from combining fracture-mechanics-based models with experimental data

Chen and Teng [24] accumulated the test results from their experiments, 27 of FRP and 23 of steel as strengthening materials, to predict by models reported by other researchers and observed that the predicted values did not fit well with the test results as shown in Table 5. Consequently, they proposed a new model to represent the relationship of bond strength.

From Table 5 it has shown that the first four models show the abundantly underestimated bond strength because the effective length is not considered while the fifth and sixth models give more reasonable results. However, Khalifa's model [13] still have drawback greater than Neubauer and Rostásy's model [10] since the greater coefficient of variation and the underestimated bond strength. Another drawback of Neubauer and Rostásy's model [10] is using of the average surface tensile strength of the concrete from the pull-off (f_{ctm}), which obtained from particular test, instead of the readily parameter as concrete strength (f_c').

Table 5 Bond strength ratio between test results to predicted results [24]

Source of model	FRP plates			Steel plates			All plates		
	Ave	Std	CoV %	Ave	Std	CoV %	Ave	Std	CoV %
Hiroyuki and Wu [3]	2.87	0.95	33	3.85	1.18	31	3.24	1.09	34
Tanaka [4]	2.92	1.65	56	5.51	5.30	96	4.02	3.96	99
Van Gemert [11]	2.19	1.12	51	1.64	0.57	35	1.91	0.96	50

Source of model	FRP plates			Steel plates			All plates		
	Ave	Std	CoV %	Ave	Std	CoV %	Ave	Std	CoV %
Chaallal et al. [12]	1.81	0.89	49	1.68	0.70	42	1.71	0.79	46
Khalifa et al. [13]	1.07	0.24	23	0.76	0.26	34	0.93	0.29	31
Neubauer and Rostásy[10]	0.82	0.15	18	0.65	0.09	13	0.74	0.15	20
Chen and Teng [24]	1.05	0.18	17	0.94	0.11	12	1.00	0.16	16

Remark Ave = Average, Std = Standard deviation, CoV = Coefficient of variation

Accordingly, Chen and Teng proposed the modified model from Yuan et al. model [9] under the following assumption;

- Use the triangular shear-slip model in Figure 2b as the representation model instead model in Figure 2d because the typical slip values at peak shear stress (δ_1) is 0.02 mm smaller than δ_f , where δ_f is 0.2 mm.
- The stress distribution is non-uniform across the section of concrete member because the effect of b_p and b_c. If the b_p is smaller than b_c, it causes greater shear stress at interfacial at failure and leads to non-uniformity in stress distribution across the width of concrete member.

Therefore, the model is proposed as follows;

$$P_u = 0.427\,\beta_p \beta_L \sqrt{f_c'}\,b_p L_e \quad , N \qquad (2.13a)$$

$$\beta_L = \begin{cases} 1 & \text{if } L \geq L_e \\ \sin[\pi L/(2L_e)] & \text{if } L < L_e \end{cases} \qquad (2.13b)$$

$$\beta_p = \sqrt{\frac{2-b_p/b_c}{1+b_p/b_c}} \qquad (2.13c)$$

$$L_e = \sqrt{\frac{E_p t_p}{\sqrt{f_c'}}} \quad \text{, mm} \qquad (2.13d)$$

which fc' = the compressive strength of cylinder concrete at 28 days. (MPa)

$E_p t_p$ is in MPa

L_e, b_p are in mm

Rewrite the equation 2.13a to be the term of the stress in the boned plate at failure by substituting equation 2.13d and $\sigma_{db} = P_u/(b_p t_p)$;

$$\sigma_{db} = 0.427\ \beta_p \beta_L \sqrt{\frac{E_p \sqrt{f_c'}}{t_p}} = 0.4 \beta_p \beta_L \sqrt{\frac{E_p \sqrt{f_{cu}}}{t_p}} \qquad (2.14)$$

where, f_{cu} = the compressive strength of cube specimen which is $1.25 f_c'$

From equation 2.14, when the bonded plate attained the high stress is desired, a high modulus of elasticity and a small thickness of the bond plate should be necessary. The ratio of the stress in the plate at failure to the tensile strength of plate is presented by

$$\frac{\sigma_{db}}{f_p} = \frac{0.427\ \beta_p \beta_L}{E_p \varepsilon_p} \sqrt{\frac{E_p \sqrt{f_c'}}{t_p}} = \frac{0.427\ \beta_p \beta_L}{\varepsilon_p} \sqrt{\frac{\sqrt{f_c'}}{E_p t_p}} \qquad (2.15)$$

From equation 2.15, when comparing two types of FRP that have close ultimate strain, the thin plate with a low elastic modulus should be manipulated for making the better tensile strength of the bond plate while the required strength is also accomplished.

2.3.2 Derivation from Simple Equation corresponding to Experimental Data

Dong-Suk Yang et al. [14], presented the interfacial bond behavior between CFRP plates and concrete from shear test (Figure3) which performed two parameters;

compressive strength (21 MPa and 28 MPa) and different bonding length (10,15, 20 and 25 cm). Many strain gages were attached on the CFRP as shown in Figure 4 in order to measure strains during load test. The effective bond length and interfacial bond-silp model could be defined and concluded as the following;

1. The effective bond length corresponding with the compressive strength was estimated by the linear regression analysis. It had been shown that the effective bond length as 200 mm was suitable.

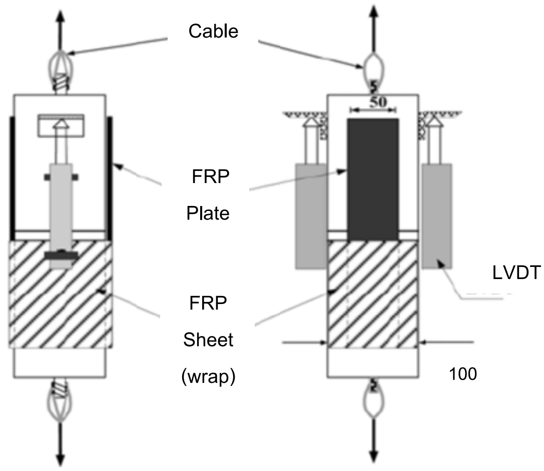

Figure 3 Loading of Specimen [14]

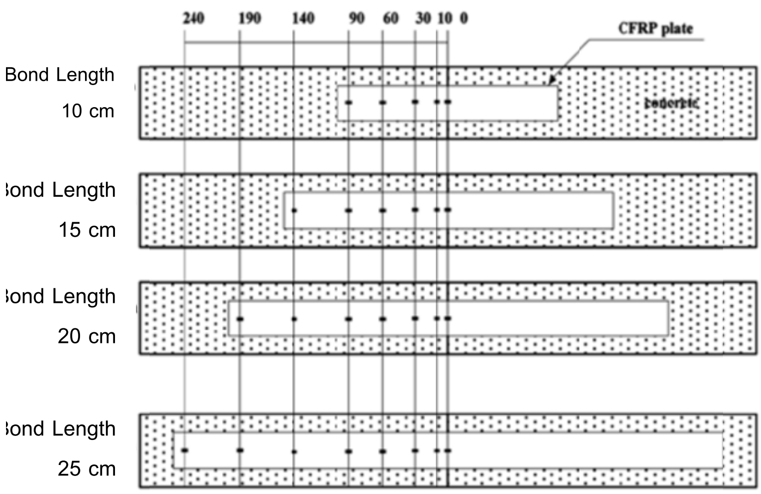

Figure 4 Location of Strain Gauses (mm) [14]

2. All specimens were failed with the debonding failure. Four from eight specimens were selected to draw bond stress-slip model because the tested bond

length was more than the effective bond length. Accordingly, the concentrated bond stress at the load end point was observed and the strain increased uniformly at the initial loading stage (Figs. 6 and 7).

From Figure5, formation of bond stress originated from equilibrium equation is

$$A_c df_c + A_f df_f = 0$$

$$\tau_b = h_f \frac{df_f}{dx} = h_f E_f \frac{d\varepsilon_f}{dx}$$

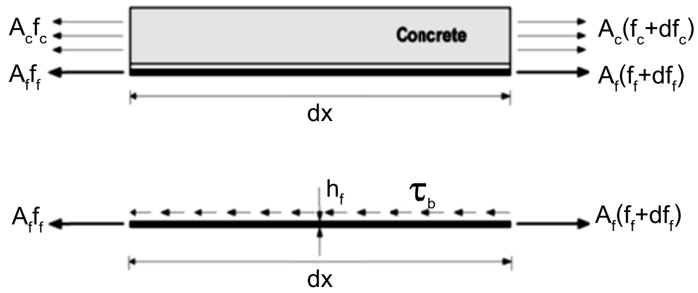

Figure5 Free body diagram between CFRP and concrete joint [14]

Assume the strain equation by the second-order equation;

$$\varepsilon_s = \varepsilon(x) = a_i + b_i x + c_i x^2$$

Then, $$\tau_{bi}(x) = h_f E_f (b_i + 2c_i x) \qquad (2.16a)$$

And slip is given by

$$\delta_i(x) = \delta_{i-1}(x) + \int_{x_{i-1}}^{x_i} (a_i + b_i x + c_i x^2)dx \qquad (2.16b)$$

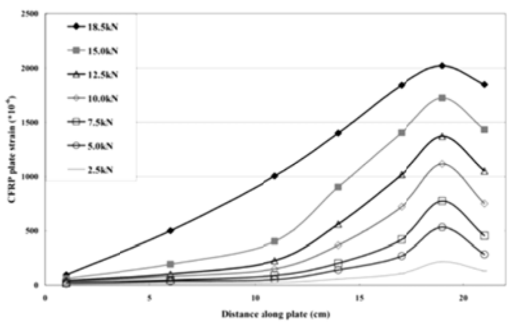

(a) D21-20 specimen

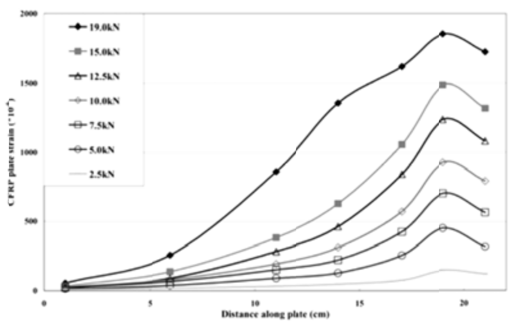

(c) D28-20 specimen

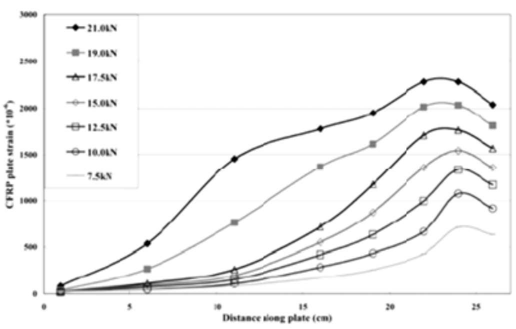

(b) D21-25 specimen

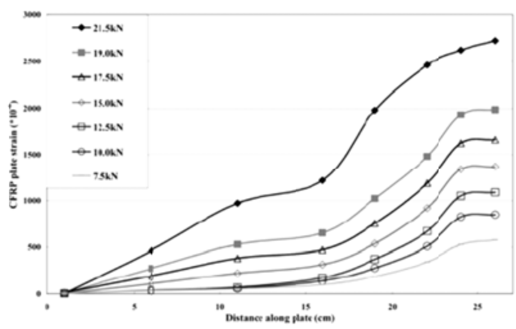

(d) D28-25 specimen

Figure 6 Strain distribution of effective bond length 20 and 25 cm [14]

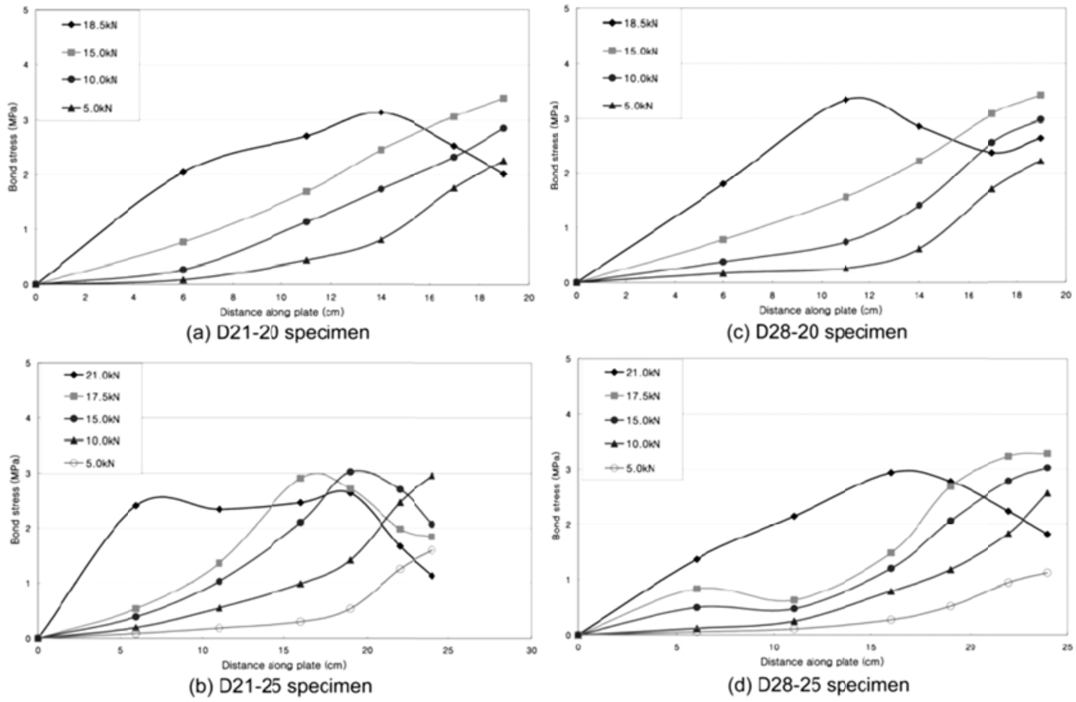

Figure 7 Bond stress distribution of specimens [14]

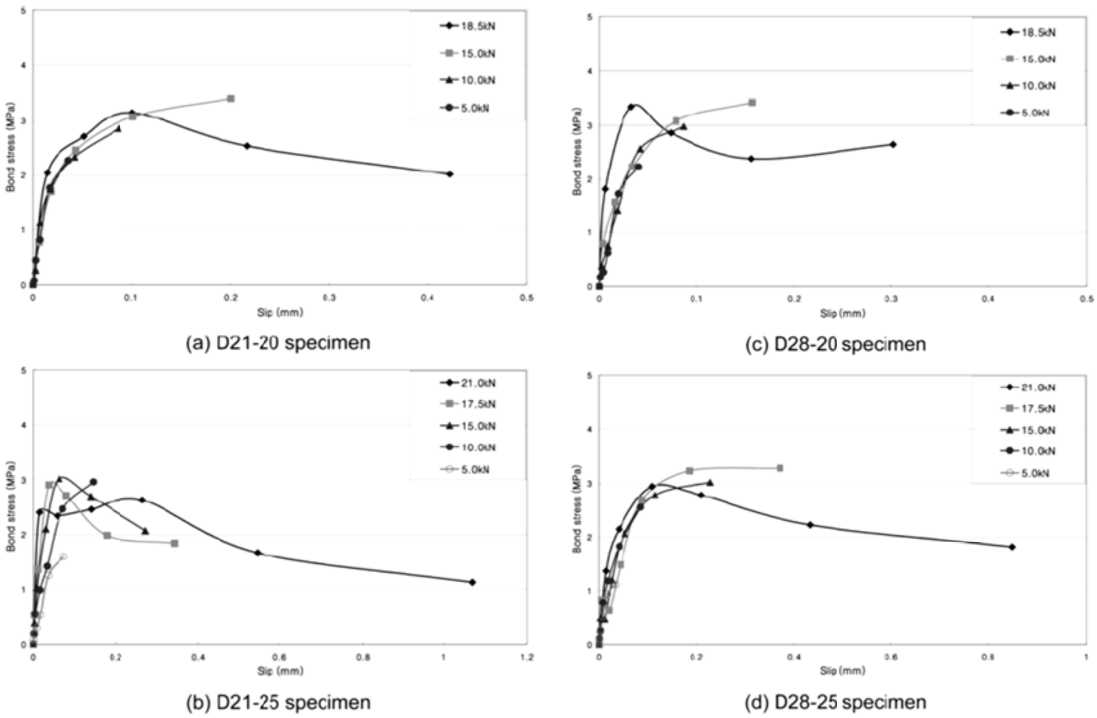

Figure 8 Bond stress and slip relations [14]

Consequently, maximum bond stress was estimated from the equation 2.16a as about 3.0-3.3 MPa

3. It could be observed that the average bond stress was equal to 1.86-2.04 MPa and the magnitude of slip between CFRP and concrete that defined as a relative slip given from difference between the concrete and CFRP plate was about 1.45-1.72 mm. Finally, the value of G_f could be found as 1.35-1.71 N/mm as shown in

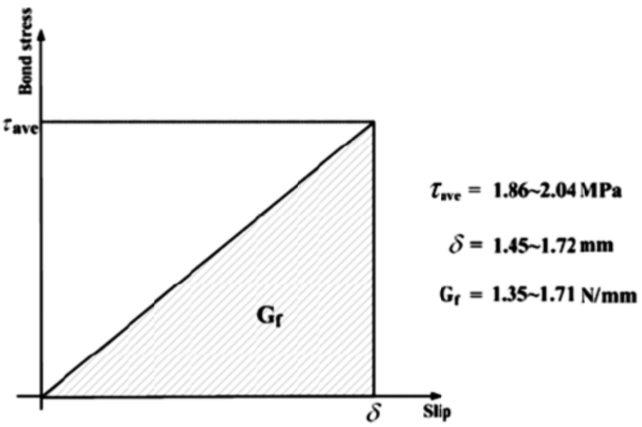

Figure 9 The prediction of bond-slip model [14]

2.3.3 Derivation of Bond-Slip Model from Simple Method [15]

Jianguo Dai et al. [15], proposed an alternative way to produce the interfacial shear stress –slip model (τ-S model) based on the relationship between pullout loads and slip at the loaded end instead of using strain distribution. This method eased the difficulty of arranging many strain gages on short effective lengths. Two parameters were varied in this study; three types of FRP (carbon, glass and aramid), four adhesive types (including primer) and derivation of τ-S model is shown as follows;

Using the stiffness (G/t) represented elastic modulus and bond layer

$$\frac{G_a}{t_a} = \frac{G_p G_{ad}}{G_p t_{ad} + G_{ad} t_p}, G_p = \frac{E_p}{2(1+\gamma_p)}, G_{ad} = \frac{E_{ad}}{2(1+\gamma_{ad})} \qquad (2.17a)$$

Where, G_a = Shear modulus of adhesive layer

t_a = Thickness of adhesive layer

E_p, E_{ad}	= Elastic modulus of primer and adhesive
t_p, t_{ad}	= Thickness of primer and adhesive
γ_p, γ_{ad}	= Poisson of primer and adhesive

<u>Methodology of analysis on test result</u>

The shear-slip relationship could be drawn based on a single-lap pullout test (Figs. 10 and 11) by

$$\tau_i = \frac{E_f t_f (\varepsilon_i - \varepsilon_{i-1})}{\Delta x} \tag{2.17b}$$

and

$$s_i = \frac{\Delta x}{2}\left(\varepsilon_0 + 2\sum_{j=1}^{i-1} \varepsilon_j + \varepsilon_i\right) \tag{2.17c}$$

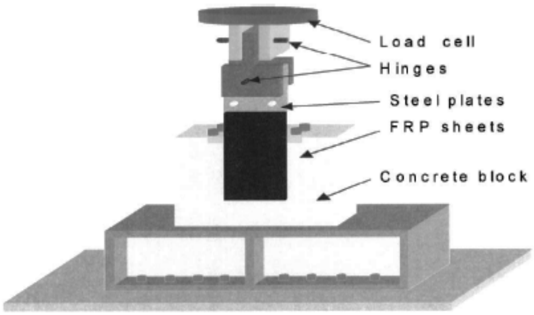

Figure 10 Single-lap pullout test [15]

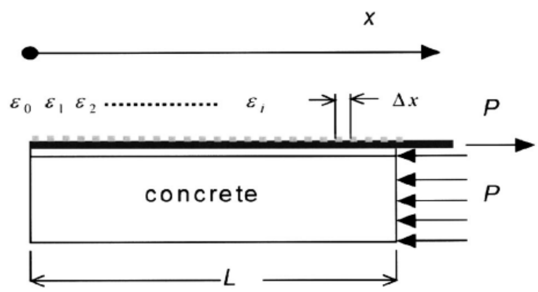

Figure 11 Detail of loaded specimen [15]

Figure 12 Strain distribution of specimen [15]

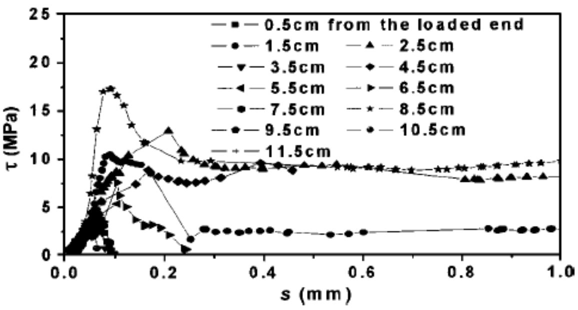

Figure 13 Stess-slip curve at different locations from loaded end [15]

From Figure13 there was a big scatter of shear stress-slip at different locations so it is not convincing to select one as representation of all. The analytical method was improved by using experimental result from former researches to define interfacial τ-S model.

Strain-slip at loaded end relationship from the simple pullout test;

$$\varepsilon = f(s) = A(1 - e^{-Bs}) \tag{2.17d}$$

From; $\frac{d\varepsilon}{dx} = \frac{df(s)}{ds}\frac{ds}{dx} = \frac{df(s)}{ds}\varepsilon = \frac{df(s)}{ds}f(s)$

$$\tau_i = E_f t_f \frac{d\varepsilon}{dx} = E_f t_f \frac{df(s)}{ds} f(s)$$

So; $$\tau = A^2 B E_f t_f \, e^{-Bs}(1 - e^{-Bs}) \tag{2.17e}$$

The interfacial fracture energy defined as

$$G_f = \int_0^{\infty} \tau \, ds = \frac{1}{2} A^2 E_f t_f$$

$$A = \sqrt{\frac{2G_f}{E_f t_f}} \tag{2.17f}$$

From theoretical approach, maximum interfacial pullout identified as

$$P_{max} = b_f E_f t_f \varepsilon_{max} = b_f E_f t_f \lim_{S\to\infty} A(1 - e^{-Bs}) = b_f E_f t_f A$$

$$P_{max} = b_f\sqrt{2E_f t_f G_f} = (b_f + 2\Delta b_f)\sqrt{2E_f t_f G_f} \tag{2.17g}$$

While Δb_f = 3.7 mm account for diminishing bond width's effect (Sato et al. [15])

Substituting equation 2.17f into equation 2.17e;

$$\tau = 2BG_f(e^{-Bs} - e^{-2Bs}) \tag{2.17h}$$

Let, $$\frac{d\tau}{ds} = -2B^2 G_f(e^{-Bs} - 2e^{-2Bs})$$

So, $$s_{max} = \frac{\ln 2}{B} = \frac{0.693}{B} \tag{2.17i}$$

$$\tau_{max} = 0.5BG_f \tag{2.17j}$$

Noted that, E_f = Elastic modulus of FRP

t_f = Thickness of FRP

A,B = The regressing parameters used for the relation between the strain of FRP sheet and slip at loaded end of bond area

τ_{max} = Maximum bond stress

s_{max} = Slip corresponding to the maximum bond stress

G_f = The interfacial fracture energy

Therefore, the equation 2.17h can represent τ-S model which depends on two parameters as B and G_f. Finally, these two parameters considered the effects of all interfacial materials such as properties of concrete, adhesives and FRP stiffness. The expression of B and G_f are given as;

$$G_f = 0.446\left(\frac{G_a}{t_a}\right)^{-0.352} f_c^{0.236}(E_f t_f)^{0.023} \quad (2.17k)$$

$$B = 6.846(E_f t_f)^{0.108}\left(\frac{G_a}{t_a}\right)^{0.833} \quad (2.17l)$$

According to above analysis, the following conclusions could be drawn.

1. Parameter B from equation 2.17l was defined as index of ductility of τ-S relationship which mainly affected from adhesive. When B was decreased, it reduced interfacial stiffness and influenced to greater ductility as shown in Figure14.

2. Parameter G_f from equation 2.17k was affected from shear stiffness of FRP and concrete strength.

3. When shear stiffness of adhesive was decreased, the ductility and interfacial fracture energy could be improved while maximum shear stress was deficiently. Although maximum shear stress was decreased, the interfacial load transfer capacity was enhanced.

4. The effect of FRP stiffness was insignificant.

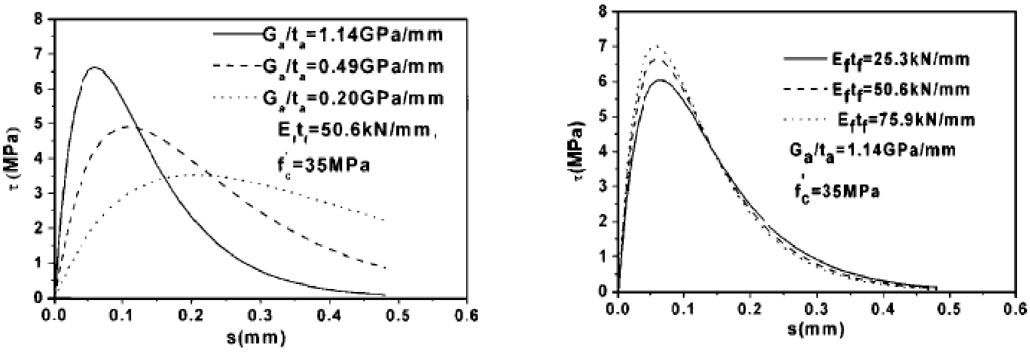

(a) (b)

Figure 14 Shear stress-slip relationship (a) with different adhesive (b) with different FRP stiffness of specimen [15]

2.4 Fire Load Concept

Ingberg [16], described the method for creating the standard of fire curve called "Fire Load Concept" and concluded the main assumptions as follows;

1. Fire resistance of structure is relied on *fire severity* which can be observed from the area under temperature and fire exposure time curve.

2. Fire severity is depended on the intensity of fire.

The assumption above does not take into account of open section area of structures, types and weights of fuel.

2.5 Basic Theory of Fire Severity [17]

There are many factors influence to fire severity. The important ones are fuel and open section area in the structure but both factors are not commonly used in analysis of fire severity because of their variability. On the other hand, damage to structure is mainly dependent on the heat absorbed by the structural elements. So the severity of fire is usually defined as the period of exposure to the standard test fire.

Fire severity is thermal energy that is released to demolish the fire resistance of materials and represented by the area under the exposure time to temperature of standard fire test. In reality, the real fires are different from the standard fire curve so the equivalent time of a complete burnout can be defined instead of designing of fire severity. The equivalent time of a complete burnout is the time of exposure to standard fire that results in an equivalent impact on a structure.

2.6 Standard Temperature-Time Curve [17]

Standard Temperature-time curve is the curve used in fire resistance tests. One of the most widely fire resistance specification test is ASTM E119 [17] (Figure 15) which is referenced in this study.

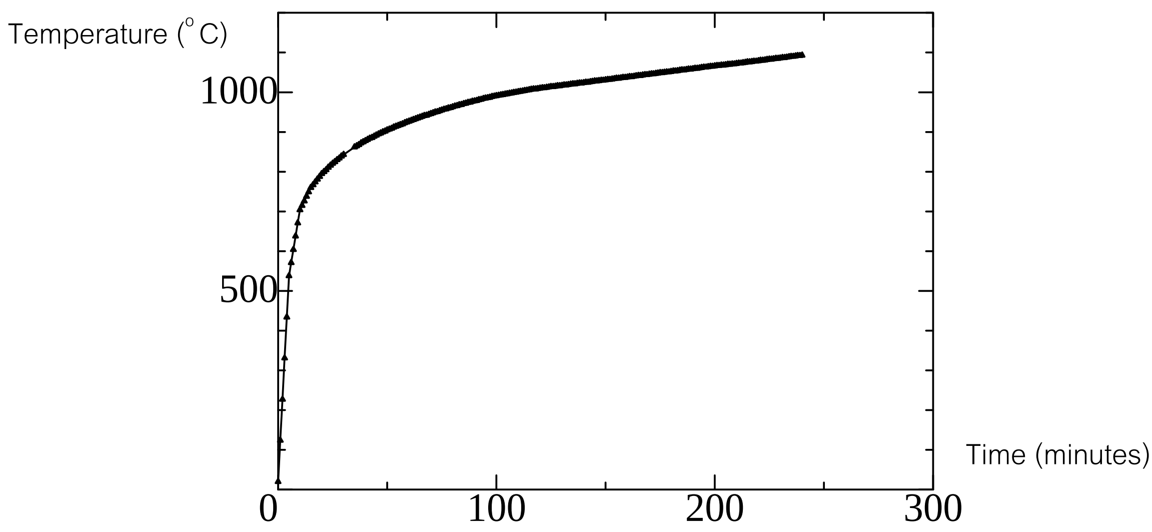

Figure 15 Standard Temperature-Time Cuve of ASTM E 119-98 [17]

2.7 Effect of Fire on Concrete

Arioz [18] studied the effect of elevated temperatures on the physical and mechanical properties of varying mixed concrete. Test procedure was varied the elevated temperature from 200 to 1200 °C and determined the compressive strength after exposure. Test result showed that the compressive strength of concrete decreased beyond to higher time exposures. From visual observation of the sample subjected to fired exposure, there were not any surface cracks at 400 °C but the color of surface specimens changed because free water in concrete started to drive out. Afterward the surface cracks became visible and increased extremely when the temperature rising to 1000°C. Finally the specimens were completely lost their bond at temperature reached to 1200°C as shown in Figure16.

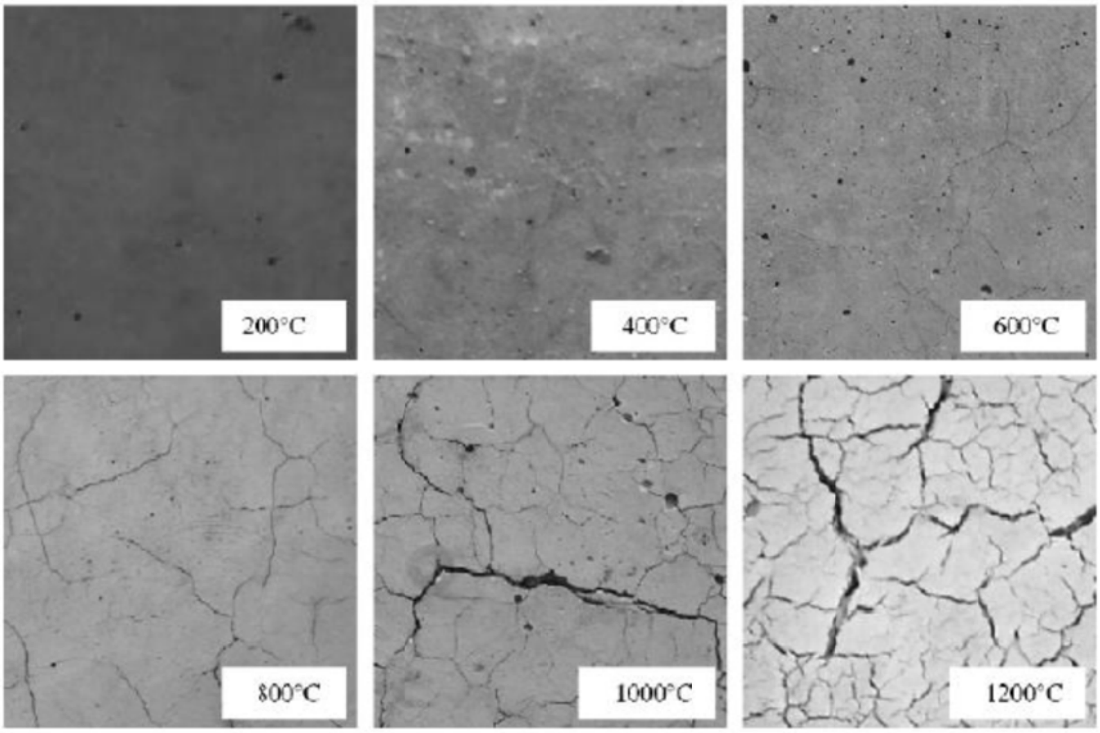

Figure 16 Characteristic of Surface Concrete Crack under Different Fire Exposures [18]

Ellingwood and Lin [19] examined the flexural strength and shear strength in reinforced concrete structure under fire exposure including the effect of concrete covering and type of fire curve. From the result, all of specimens failed by flexural failure and the concrete covering barely affected to deflection of beam. This means that the resisting shear strength is not a control parameter when the temperature rises up. Furthermore, using different fire curve also influence to temperature distribution in the RC member.

Hansanti [20] studied the effect of time exposure to the compressive strength, tensile behavior of reinforcing steel, bond strength between concrete and reinforcing steel, shear and flexural behavior of RC beam and appropriate method for performance evaluation by non-destructive test. From the experiment, the following conclusions can be drawn.

1. The value of compressive strength in concrete specimens decreased with a higher exposure time and related to the velocity from ultrasonic pulse velocity test.

2. A concrete covering played an important role on reinforcing steel behavior after fire exposures because it was a protection against fire. Moreover, it was shown that the proper covering to protect the reduction in tensile strength of reinforcing steel is 25 mm for exposure time lower than 90 minutes. And, the elastic modulus did not changed significantly.

3. The bond strength between reinforcing steel and concrete after fire had a reverse relation with time exposure and influenced in the round bar more than deform bar.

4. The tendency of shear strength reduced 10 percents per 30 minutes (the exposure not longer than 60 minutes) by compared with ACI 318 shear strength specification. However, the shear strength by ACI 318 still has the value of safety factor as 1.23 at 60 minutes exposure.

5. The specimens under fire exposure less than 60 minutes had no effect on the yield and ultimate moment of beams. On the contrary, it had an effect when the fire exposure reached to 90 minutes by the yield and ultimate moment declined as 16 and 15 percents, respectively.

CHAPTER III

Research Methodology

In this chapter, research methodology which consists of several processes is described as following;

3.1 Literature review

The variety of reinforced concrete members strengthened with FRP was reviewed for instant several kind of bonding tests and a number of interfacial bond –slip models. Moreover, the effect of fire on concrete also was considered.

3.2 Preparing test specimens

1. Designing concrete mix proportion which had the cylindrical compressive strength (fc') equal to 240 ksc and 350 ksc for ensuring the failure on the 240-ksc beam.

2. Mixing concrete operated under ASTM C192/C 192M-07 "Standard Practice for Making and Curing Concrete Test Specimens in The Laboratory" [21].

3. The slump test was taken follow ASTM C143/C143M-08 "Standard Test Method for Slump of Hydraulic Cement Concrete" [21].

4. Concrete were molded into cylindrical and rectangular size of 10x10x50 cm^3 and specimens were cured for 28 days as shown in Figs. 18-21 while at top face of specimens that varied covering would be the fire exposure surface. Accordingly, 25 sets of rectangular specimen having detail as shown in Table 10 were reinforced with DB12 steel at 4 corners and RB6 as stirrup to prevent tension and flexural damages as shown in Figure 17.

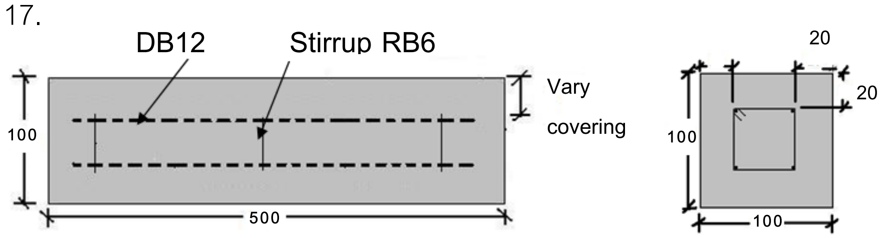

Figure 17 Dimension of Specimens

Table 6 Detail of all specimens varying with different parameters

Name of Specimens	Covering (cm)	Exposure Time (min)	Bond Length (cm)	Quantity
1C0-15	1	0	15	1
1C0-20	1	0	20	1
1C0-30	1	0	30	1
2C0-15	2	0	15	1
2C0-20	2	0	20	1
2C0-30	2	0	30	1
3C0-15	3	0	15	1
3C0-20	3	0	20	1
3C0-30	3	0	30	1
1C45-15	1	45	15	1
1C45-20	1	45	20	1
1C45-30*	1	45	30	-
2C45-15	2	45	15	1
2C45-20	2	45	20	1
2C45-30	2	45	30	1
3C45-15	3	45	15	1
3C45-20	3	45	20	1
3C45-30*	3	45	30	-
1C90-15	1	90	15	1
1C90-20	1	90	20	1
1C90-30	1	90	30	1
2C90-15	2	90	15	1
2C90-20	2	90	20	1
2C90-30	2	90	30	1
3C90-15	3	90	15	1
3C90-20	3	90	20	1
3C90-30	3	90	30	1
Total specimens				25

Note: CCT-BL represents the number of all specimens while C = concrete covering (1, 2 or 3 cm), T = exposure time (0, 45 or 90 minutes) and BL = bond length (15, 20 or 30 cm)

* = lack of specimen for attached CFRP because the excessive damage occured on the specimen surface.

Figure 18 Cylindical Mold

Figure 19 Rectangular Mold size of 10x10x50

Figure 20 Molding ConcreteSpecimen

Figure 21 Curing Concrete specimens

5. The specimens were fire in the oven (Figure 22) with difference exposure time under ASTM E119-10 “Standard Test Methods for Fire tests of Building Construction and Materials”.

6. Before the burn process, all specimens had to wrap with ceramic fiber to protect concrete surface from flame except in the top surface which are the face that exposed to fire exposure and varied covering as shown in Figs. 23 and 24.

Figure 22 Concrete oven for stimulate flame

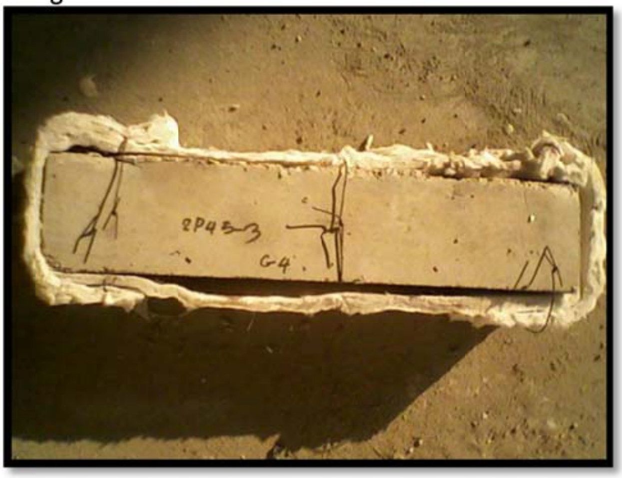

Figure 23 Wrapped specimen with ceramic fiber for prevention of flame onto concrete surface

Figure 24 Burnt specimens at exposure time of 90 mins

7. After removal fired specimens from the oven and dried out at room temperature, the direct tension (Pull-off Method) testing was taken on damaged surface by using ASTM C1538/C1538M-04 Standard test method for tensile strength of concrete surfaces and the bond strength or tensile strength of concrete repair and overlay materials. The process of Pull-off test are performed as following in Figure25

(a) Leveling concrete surface

(b) Chipping off concrete surface to size of 5x5 cm.

(c) Attached the steel disk by epoxy

(d) Measuring surface tensile strength by tensile loading device

e) The appearance of damaged concrete after pull-off testing

Figure 25 Means of pull-off testing

8. Design effective bond length of CFRP plate to concrete joint referenced from the technical report of FIB (fédération internationale du béton). In this research, the effective bond length equal to 20 cm. Moreover, 15 and 30 cm were adopted as other bond lengths. The properties of CFRP plate are shown in table 11

9. Installed FRP on prepared reinforced concrete specimens under the standard of the department of public works and town & country planning (DPT 1508-51 standard). However, before CFRP plates were attached on several specimens, all rectangular beams were manipulated as following;

1) Measure dimension of all specimen and paired concrete between burnt specimen and controlled specimen. Adjusting elevation of paired concrete specimens to prepare for attaching CFRP plate.

2) Bonded CFRP plate on damaged surface with the designed bond length. The properties of CFRP plate and adhesive are shown in table 7 and 8 and the picture of FRP installation are shown in Figure 26

Table 7 Properties of CFRP plate

Material	Elastic modulus (N/mm^2)	Tensile strength (N/mm^2)	Section (mm^2)
Sika® CarboDur® type S	165000	2800	1.2x50

Table 8 Properties of Adhesive

Material	Elastic modulus (N/mm^2)	Poisson's ratio
Sikadur®-30	165000	0.22
Sikadur®-31	4150	0.45

Figure 26 Attaching CPRP plate on concrete surface

3.3 Testing procedures of modified pull-out test

After attaching CFRP onto damaged concrete surface, the modified pull-out test was performed to investigate the interfacial bond strength between FRP and concrete after fired exposure as detailing;

1. Many strain gages were attached with 20 mm interval from loaded end on CFRP plate as shown in Figure 27

2. The prepared specimens are installed to the modified pull-out test. The model of testing machine was originated from Kobayashi et al. [23] The bond test machine has separable 2 H-shape steel beams at the base of the testing machine that are jointed together with hinge for allowable only tensile force in the specimen as shown in Figs. 28 and 29.

3. Load would be increased to the specimen until failure.

4. Collecting the value as following; Strain from stain gages and load from load cell for analyzing to propose the effect of fire on bond behavior between CFRP and damaged concrete.

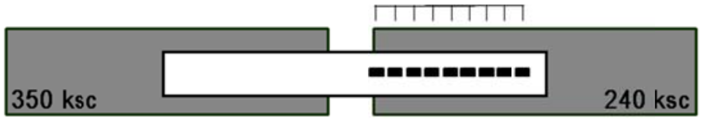

Figure 27 Detailing of strain gages on CFRP plate

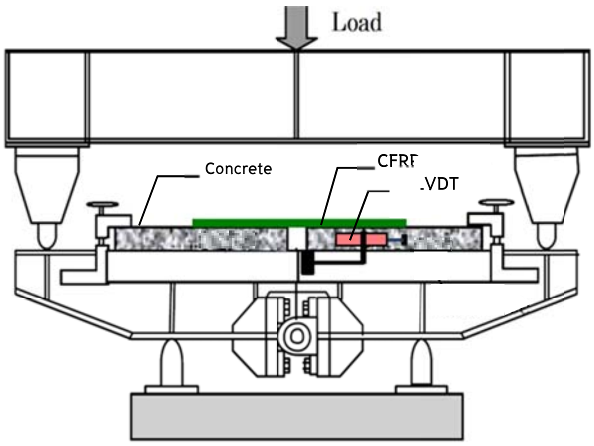

Figure 28 Modified pull-out testing machine (Drawing)

Figure 29 Loading of specimens

3.4 Empirical model implementation

1. Studied the bond behavior between reinforced concrete and CFRP through shear stress-slip relationship from others researcher.

2. Compared the collected experimental data with other researchers such as strain distribution, relationship between strain and slip of concrete and CFRP and shear stress-slip relationship.

3. Conducted the properly shear stress-slip model and modified that existing relationship correspond to the experimental results, for instance, the interfacial fracture energy or some constant parameter were adjusted for considering the effect of important parameters. Consequently, the bonding relationship between concrete and CFRP in non-fired series could be proposed.

4. Derived the shear stress-slip model of specimens under fired in the same way as described in non-fired specimens.

5. Verifying the applicability of the proposed model with the experimental data from previous study.

3.5 Flow Chart of Methodology

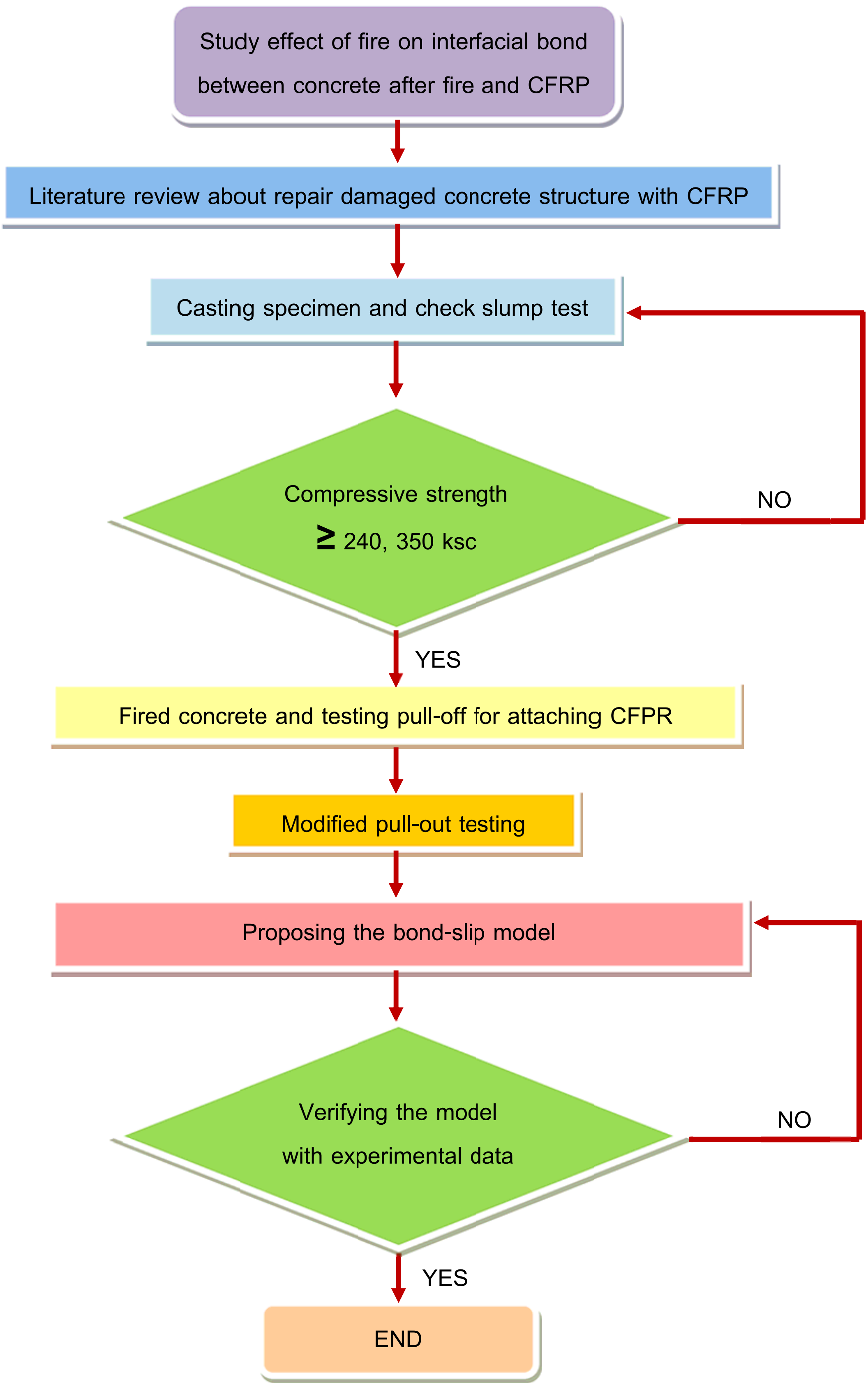

CHAPTER IV

Experimental Results and Discussions

According to chapter 3, the experimental results are performed and discussed as following;

4.1 Damaged concrete from fire and pull-off test

In this study, all specimens were exposed to 0, 45 and 90 minutes and fired specimens were conducted under standard temperature-time curve of ASTM E119 as shown in Figure 30-31 and the appearance of damaged concrete with different exposure times were compared and presented in tables 10-11 as following;

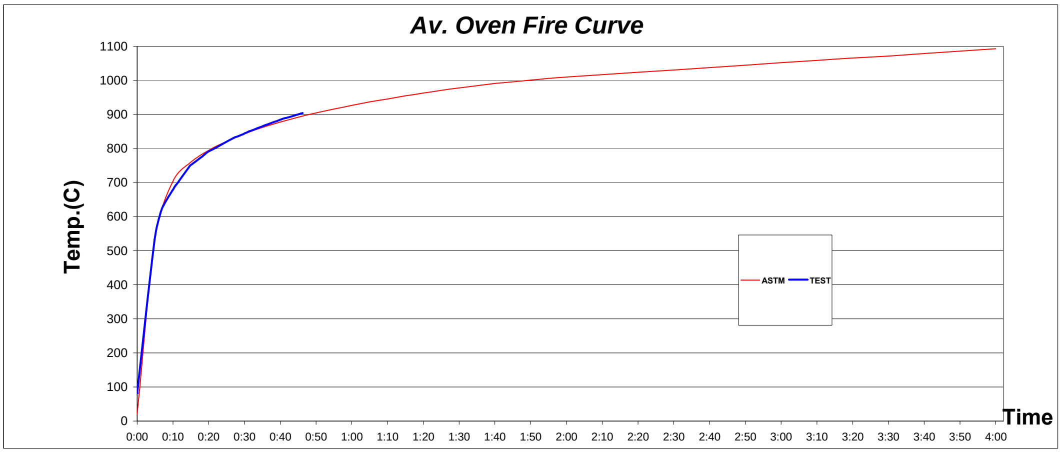

Figure30 Relationship between Temperature and Time at Exposure Time 45 min

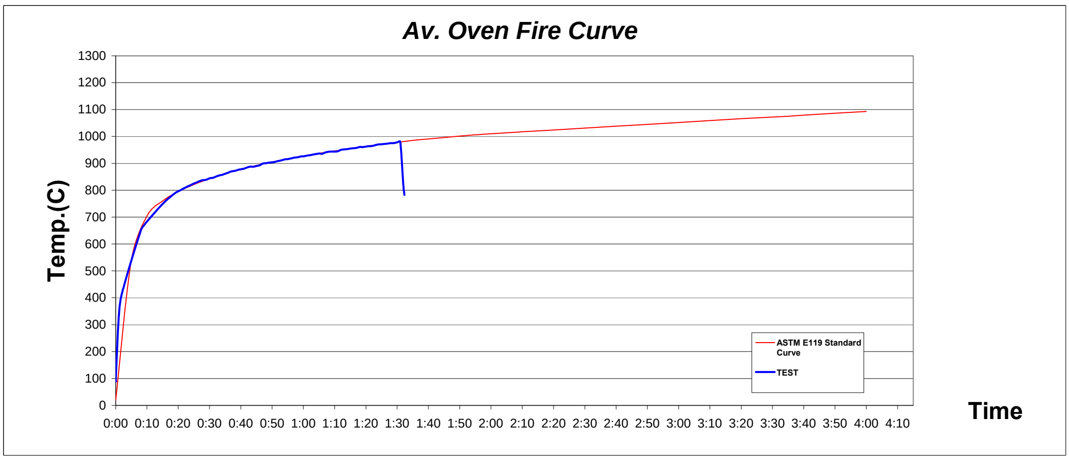

Figure31 Relationship between Temperature and Time at Exposure Time 90 min

Table 9 Appearance of Concrete Specimens (Cylinder)

Exposure time (min)	Appearance of Concrete Specimens (Cylinder)
0	
45	 
90	

Table 10 Appearance of Concrete Specimens (Beam of Rectangular Specimen)

After dried out the fired specimens at room temperature, the pull-off test was

Exposure time (min)	Appearance of Concrete Specimen		
	Covering 1 cm	Covering 2 cm	Covering 3 cm
0			
45	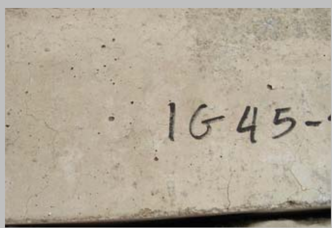 	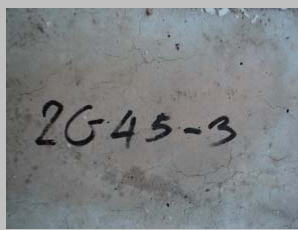 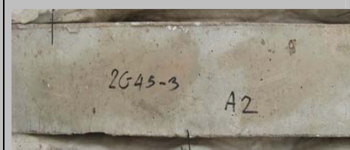	 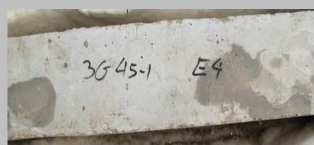
90			

done to find out the surface tensile strength of concrete corresponding to the ASTM C1538/C 1538M-04 Standard test method for tensile strength of concrete surfaces and the bond strength or tensile strength of concrete repair and overlay materials. The results of surface tensile strengths are shown in table 12.

Table 11 Result of pull-off test

Specimens	Surface tensile strength (Pull-off test) (N/mm^2)
1C0-15	1.47
1C0-20	
1C0-30	
2C0-15	1.97
2C0-20	
2C0-30	
3C0-15	2.23
3C0-20	
3C0-30	
1C45-15	0.1
1C45-20	
2C45-15	0.16
2C45-20	
2C45-30	
3C45-15	0.18
3C45-20	
1C90-15	0.11
1C90-20	
1C90-30	
2C90-15	0.16
2C90-20	
2C90-30	

Specimens	Surface tensile strength (Pull-off test) (N/mm^2)
3C90-15	0.10
3C90-20	
3C90-30	

According to tables 10 and 11, the appearance of damaged concrete changed from grey concrete to pink color and concrete material becomes softer. More dispersed spalling could be observed on concrete surface for any higher exposure time and concrete covering, especially in specimens with 90 minutes of exposure time and 3-cm covering where a burst of concrete appeared in some areas on the surface and resulted in the exposure of the reinforced steel to the environment. The severe damages may be caused by free water in concrete void that tried to evaporate out from the concrete when the pressure in the concrete covering increased due to the increased in the temperature. Furthermore, from the pull-off test results in table 12, it shows that the temperature from fire has greater effect on the surface tensile strength than the concrete covering. Therefore, the increase in the temperature will result in greater damage to the concrete's surface and also has a greater effect on the concrete's tensile strength rather than the concrete covering.

4.2 Modified pull-out test (Originated from Kobayashi et al. [23])

4.2.1. Failure mode of experiment

A number of bond tests in FRP-concrete have been continuously carried out and developed in the past, but no presenting on standard bond test. However, four generally well-known methods to examine the bond test are single shear test, double shear test, beam test and modified beam test or modified pull-out test [14]. In this study, the experiment was carried out through the modified pull-out test and the failure mode of all specimens was found out to be the debonding at concrete substrate. But in fact, there were some specimens that failed by debonding at adhesive on unexpected side (on the 350 ksc of compressive strength's side) as shown in table 13 and Fig 32.

Table 12 Results from modified pull-out test

Specimens	Interfacial bond strength (Modified beam test) (kN)	G_f (Experimental) (N/mm)	Failure mode*
1C0-15	24.75	0.1658	DC
1C0-20	23.94	0.4749	DC
1C0-30	28.89	0.5539	DA,O
2C0-15	28.98	0.4663	DC
2C0-20	28.92	0.5125	DC
2C0-30	30.49	0.6536	DC
3C0-15	26.69	0.2215	DC
3C0-20	27.44	0.4273	DC
3C0-30	27.91	0.5279	DA,O
1C45-15	13.28	0.0290	DC
1C45-20	12.86	0.0492	DC
2C45-15	8.44	0.0134	DC
2C45-20	16.59	0.0937	DC
2C45-30	19.50	0.2291	DC
3C45-15	7.04	0.0052	DC
3C45-20	15.32	0.0595	DC
1C90-15	13.33	0.0309	DC
1C90-20	12.50	0.0462	DC
1C90-30	15.38	0.1394	DC
2C90-15	8.35	0.0265	DC
2C90-20	10.68	0.0482	DC
2C90-30	16.12	0.1850	DC

Specimens	Interfacial bond strength (Modified beam test) (kN)	G_f (Experimental) (N/mm)	Failure mode*
3C90-15	8.01	0.0093	DC
3C90-20	11.25	0.0474	DC
3C90-30	20.00	0.1622	DC

Note : * DC = Debonding at concrete substrate, DA = Debonding at adhesive, O = specimen fail on unexpected side

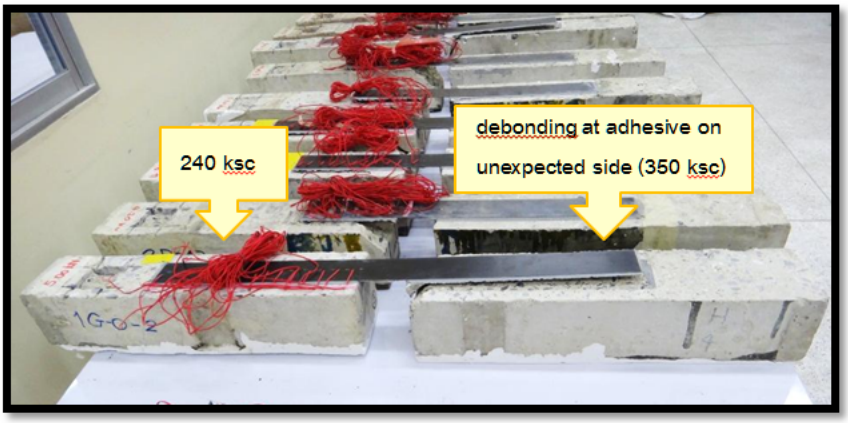

(a)

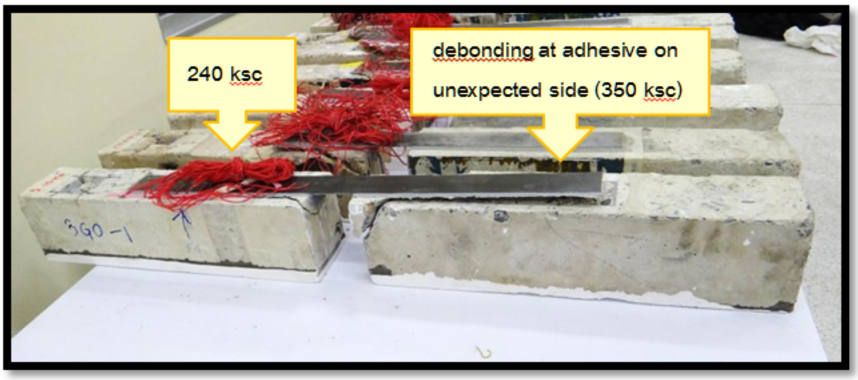

(b)

Figure32 Debonding at adhesive on unexpected side (350 ksc) of 1C0-30 and 3C0-30

4.2.2. Relationship between interfacial bond strength to all parameters

After conducted all specimens by modified pull-out test, various data were gathered from the test. One of that was an interfacial bond strength which was the value refer to bond strength between CFRP and concrete under different exposure times as shown in table 13. The effects of each parameter to this bond strength are described as following.

1) Relationship between interfacial bond strength and bond length (Pmax-BL)

According to previous researches, many researchers tried to study and develop bonding behavior of FRP to concrete. The bond length of FRP is one of the factors that influence the bonding behavior because the tensile force or interfacial bond strength will be transferred between concrete section and FRP for strengthening its structure. The bond length of FRP's concept differ from the idea of reinforced steel in RC structure where the idea of reinforced steel in RC structure shows that the tensile strength of the concrete will continuously increase according to the increase of the bond length. However, there is an existing active bonding zone called effective bond length, Le, between interface of FRP and concrete for manipulating ultimate tensile strength. Consequently, the increase of the tensile strength of the FRP's concept will reach an ultimate tensile strength at the effective bond length and thus will not increase further according to the increase in the bond length as verified from previously experimental studies and fracture mechanic analyses. Although, the longer bond length cannot progress more ultimate tensile strength but instead, it can improves the ductility of mechanism [1].

In this study, the effective bond length of CFRP was designed based on normal concrete. Three bond lengths were chosen, which are 15, 20 and 30 cm.

The 20 cm was chosen as it is the effective bond length, while 15 and 30 cm are lower and greater value than the effective bond length. From Figure33, the relationship between interfacial bond strength and bond length, the temperature from the fire could change the effective bond length in series of damaged specimen (1C45-3C45 and 1C90-3C90) because longer bond length significantly caused an increase in bond strength of the fired-specimens. While the interfacial bond strength of 20 cm and 30 of normal concrete were not much different.

2) Relationship between interfacial bond strength, exposure time and concrete covering (Pmax-T-C)

From Figure 34, the bond strengths decrease with an increase in exposure time. While the effect of concrete covering to bond strength has not clarify. Accordingly, the effect of fire has greater influence to the interfacial bond strength than concrete covering.

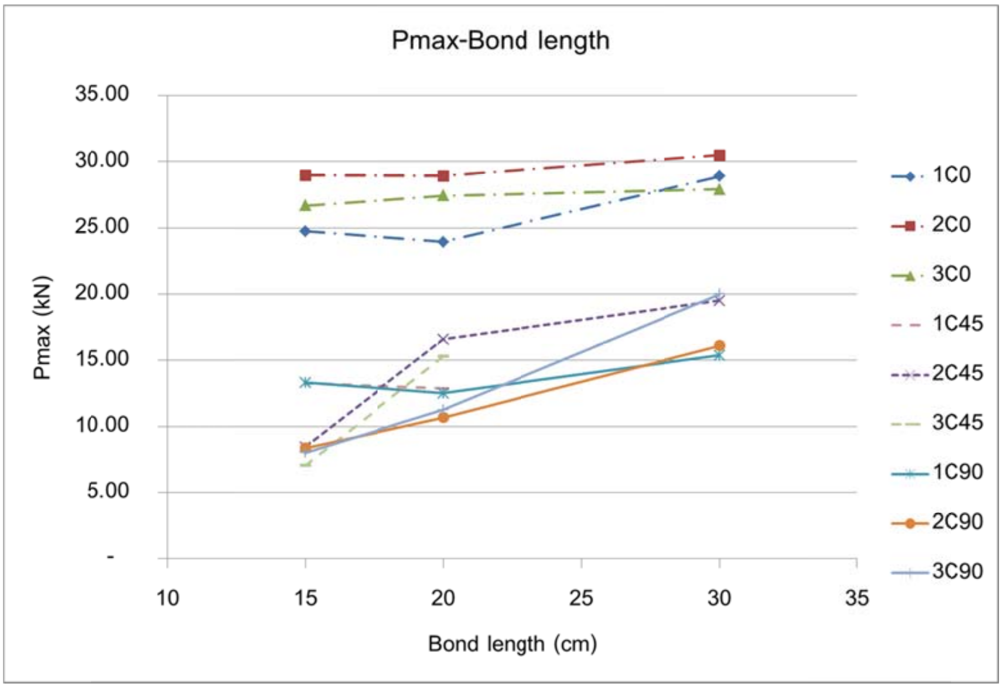

Figure33 Relationship between interfacial bond strength and bond length

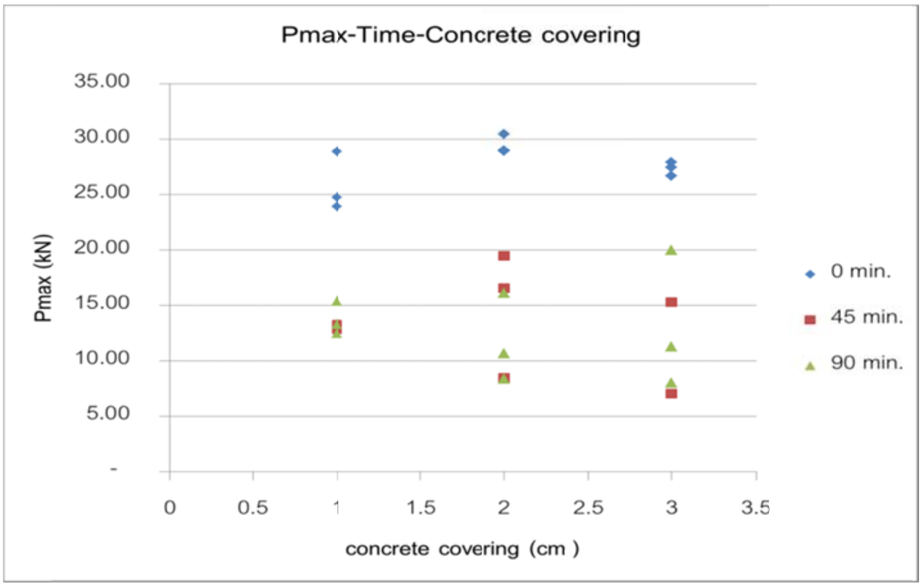

Figure34 Relationship between interfacial bond strength, Time and Concrete covering

4.2.3. Shear stress-slip curve from modified pull-out test

Moreover, the interfacial bond strength of modified pull-out test, numerous strains from all strain gages were also collected for calculating the interfacial fracture energy or G_f in order to generate the shear stress-slip model in the next topic. Generally, in order to calculate G_f from bond stress-slip curve, many strain gages are attached on the FRP with small interval for conducting the relationship between bond stress and slip at every load step. Figure 35 shows the strain distribution of strain gages along CFRP plate at every load step and the detail of modified beam test. The shear stress can be obtained from the following equation (4.1) which can be derived from the equilibrium equation

$$\tau_i = \frac{E_f t_f (\varepsilon_i - \varepsilon_{i-1})}{\Delta x} \qquad (4.1)$$

Where, τ_i = Average interfacial bond stress at the section i

ε_i , ε_{i-1} = Strain value from strain gages as shown in Figure35

E_f = Elastic modulus of CFRP plate

t_f = Thickness of CFRP plate

Δx = strain gages interval

In case of bond slip, it can be calculated from the relative displacement between concrete and CFRP. The displacement of CFRP can be computed from the following expression:

$$s_i = \frac{\Delta x}{2}\left(\varepsilon_0 + 2\sum_{j=1}^{i-1}\varepsilon_j + \varepsilon_i\right) \tag{4.2}$$

Where, s_i = local slip of the CFRP at section i

ε_0 = strain value at free-end face of CFRP plate

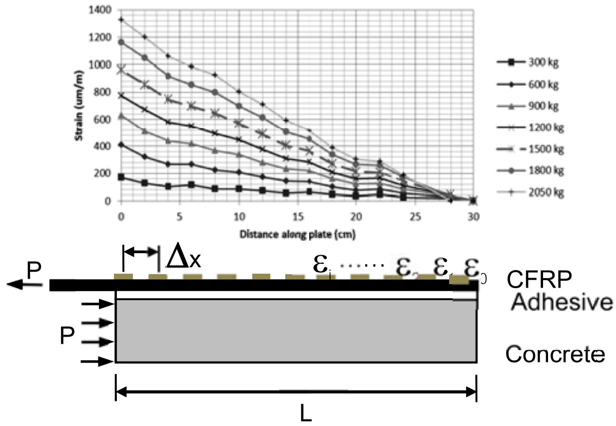

Figure35 Strain distribution of 3C90-30 along the CFRP plate in modified pull-out test

Therefore, the interfacial bond stress-slip curve could be drawn as shown in Figure 36 and the area under the curve was computed to define the G_f as shown in Table 13.

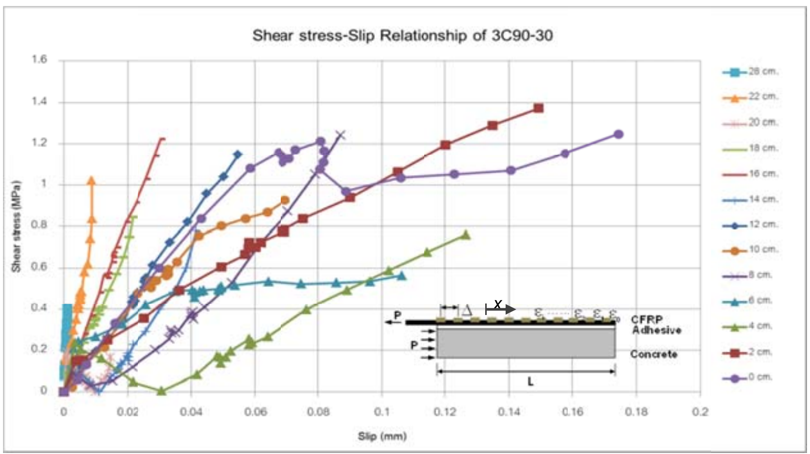

Figure36 Interfacial bond stress-slip curve of 3C90-30 at each strain location

4.2.4 Interfacial fracture energy (G_f) from modified pull-out test

The interfacial fracture energy, G_f, is an important parameter for bonding behavior which is the energy required to bring a fixed unit area to complete separation. It can be computed from area underneath the bond stress-slip curve [15]. The values of G_f are reported in the table 12 and the relationship between G_f and all parameters are shown in Figure 37-39.

According to Figure37 and 38, the variation of interfacial fracture energy is directly related to the bond length but inversely proportional to exposure time. When the temperature increases, bonding between CFRP-concrete is destroyed and result in the decrease in G_f. On the other hand, the G_f will increase with increasing bond length because the greater bond length can provide more ductility and relate to more resistance of FRP until failure.

In case of concrete covering, it obviously sees that the influence of concrete covering has the least effect to G_f when compare with all parameters as performed in Figure37, 38 and 39. However, the values of G_f from experiment still have been influenced from concrete covering but that effect has been neglected by the exposure time. From Figure39a, the effect of concrete covering shows the reverse relationship to G_f in 20 cm and 30 cm in bond length. On the other hand, when exposure time is increase, the relationship between G_f and concrete covering does not clarify and has insignificant relation as performed in Figure39b and 39c. Therefore, it can be concluded that the effect of concrete covering will be neglected when the fire temperature arises.

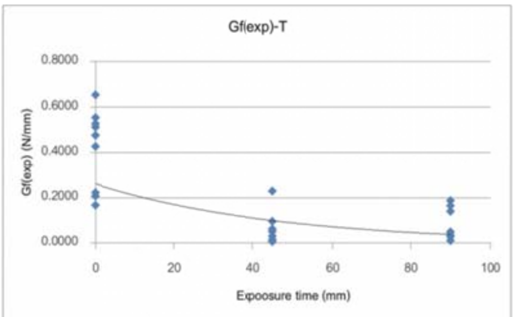

Figure37 Effect of exposure time to G_f

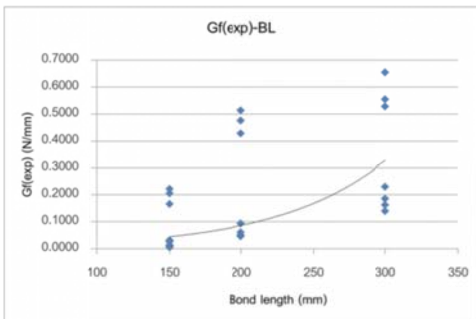

Figure38 Effect of bond length to G_f

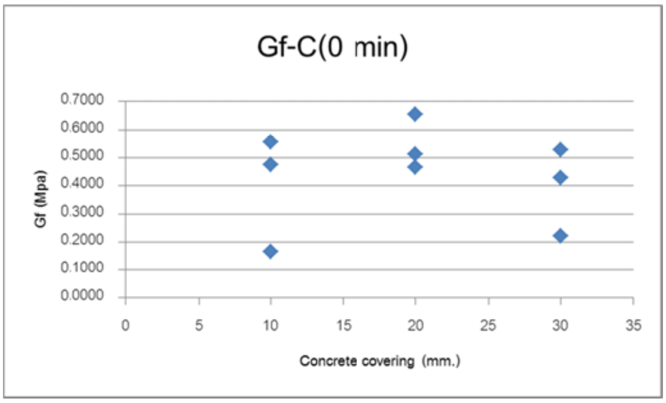

(a) Exposure time 0 min.

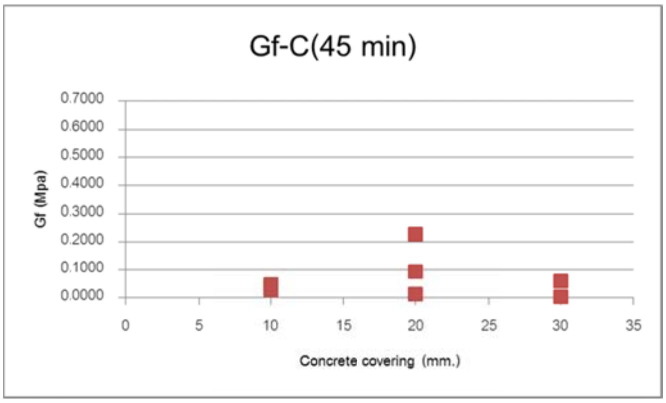

(b) Exposure time 45 min.

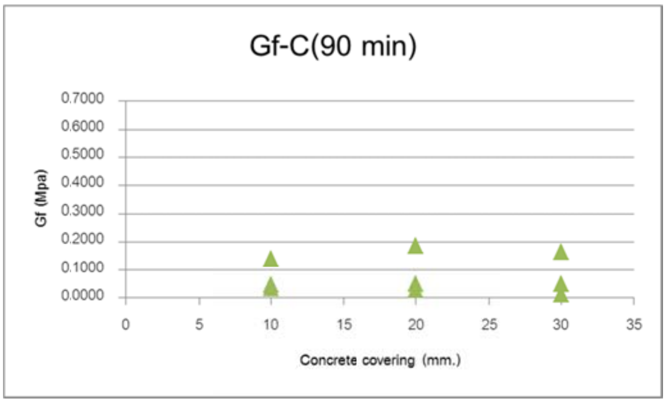

(c) Exposure time 90 min.

Figure39 Effect of concrete covering to G_f

4.3 Empirical model implementation

The empirical model implementation in this study consists of 2 parts as shown in Figure40 which was modified from the bond-slip model as expressed in chapter 2. Firstly, the important parameter, G_f, could be formulated from experimental data by including the effect of all parameters in this study. Later on, the parameter G_f was applied to develop shear stress- slip model for representing the bonding behavior between reinforced concrete after exposed fire and CFRP plate.

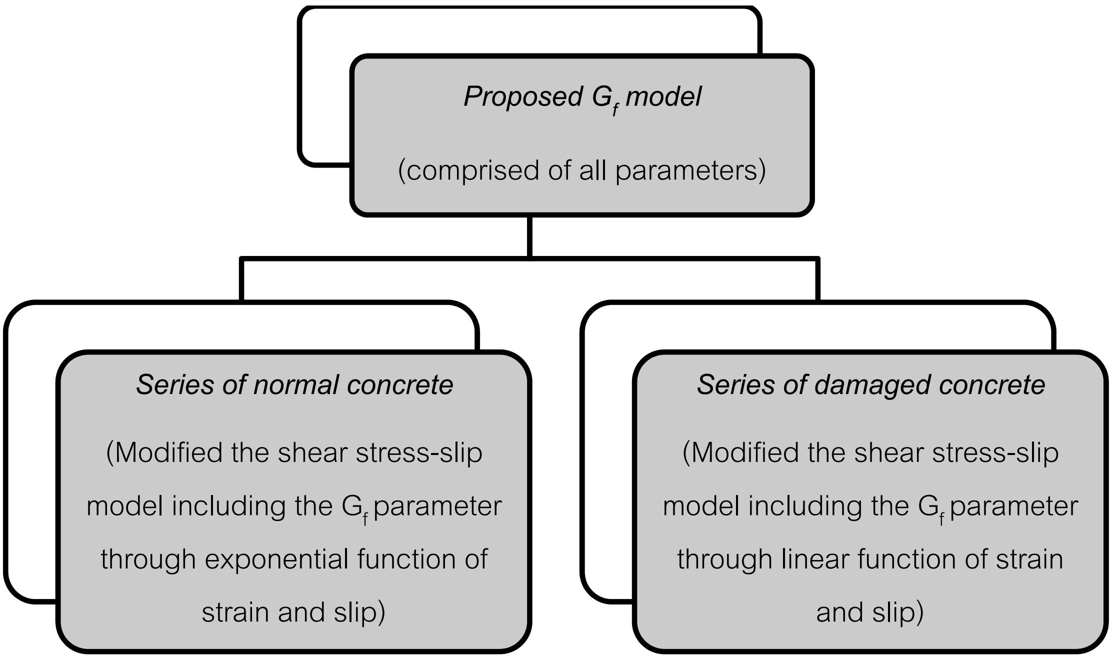

Figure40 The empirical model implementation

4.3.1 Intergration of all parameters into the interfacial fracture energy, G_f

According to the experimental data of G_f which computed from the area underneath the shear stress-slip curve, the model of G_f could be defined. However the effect of concrete covering has insignicant effect on the interfacial fracture energy as described in 4.2.4, therefore, it was not considered in this model.

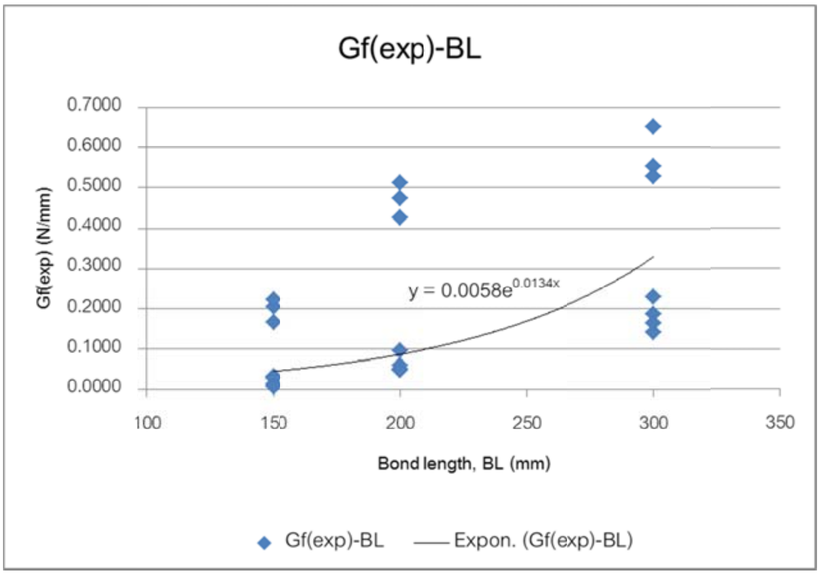

(a)

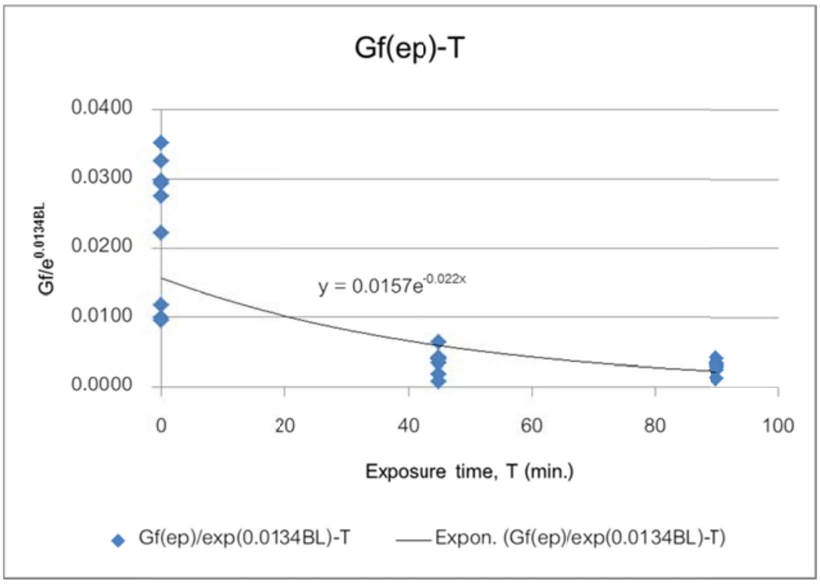

(b)

Figure41 The effect of various parameters on the interfacial fracture energy
(a) Bond length (b) Exposure time

Through the regression of the interfacial fracture energy, the parameter G_f can be expressed corresponding to various parameters as displayed in equation 4.3. The model of G_f will be appiled for developing the shear stress-slip model as described in the next topic.

$$G_f = 0.0157\, e^{0.0134BL-0.022T} \qquad (4.3)$$

Where, G_f = Interfacial fracture energy, N/mm

BL = Bond length of CFRP plate, mm.

T = Exposure time, min.

The comparisons between experimental value and predicted value of G_f can be shown in the table 14 and Figure 42

Table 13 Results of the predicted G_f and the experimental G_f

Specimens	G_f (Experimental) (N/mm)	G_f (Predicted) (N/mm)
1C0-15	0.1658	0.1172
1C0-20	0.4749	0.2290
1C0-30	0.5539	0.8745
2C0-15	0.4663	0.1172
2C0-20	0.5125	0.2290
2C0-30	0.6536	0.8745
3C0-15	0.2215	0.1172
3C0-20	0.4273	0.2290
3C0-30	0.5279	0.8745
1C45-15	0.0290	0.0435
1C45-20	0.0492	0.0851
2C45-15	0.0134	0.0435
2C45-20	0.0937	0.0851
2C45-30	0.2291	0.3249

Specimens	G_f (Experimental) (N/mm)	G_f (Predicted) (N/mm)
3C45-15	0.0052	0.0435
3C45-20	0.0595	0.0851
1C90-15	0.0309	0.0162
1C90-20	0.0462	0.0316
1C90-30	0.1394	0.1207
2C90-15	0.0265	0.0162
2C90-20	0.0482	0.0316
2C90-30	0.1850	0.1207
3C90-15	0.0093	0.0162
3C90-20	0.0474	0.0316
3C90-30	0.1622	0.1207

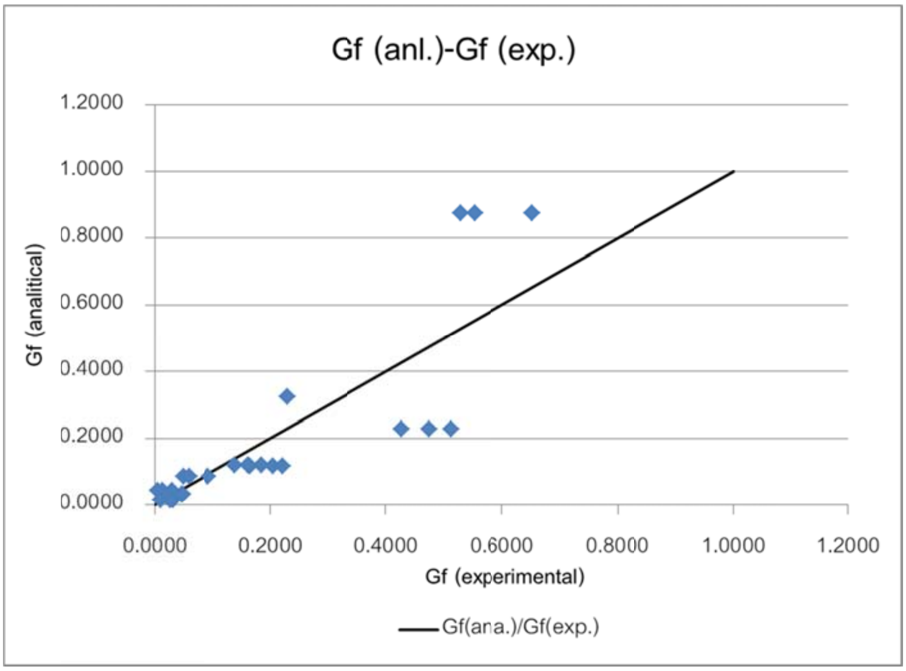

Figure42 Comparisons between experimental value and predicted value of G_f parameter

4.3.2 Relationship between shear stress-slip model of normal concrete specimens (exposure time equal to 0 min.)

According to the literature review in chapter 2, various bond-slip models were reveiwed and compared with experimental data that obtained from this study. The proper model had been seleted for improving the shear stress-slip relationship, which was Jianguo Dai et al.'s model [15]. This model was derived from simple method, single-lap pullout test. The Jianguo Dai et al.'s model was developed from strain-slip relationship at loaded end which is an exponential function as shown in equation 4.4. From the strain-slip relationship, the constant *A* and *B* are obtained as shown in Figure43 and table 15.

$$\varepsilon = f(s) = A(1 - e^{-Bs}) \tag{4.4}$$

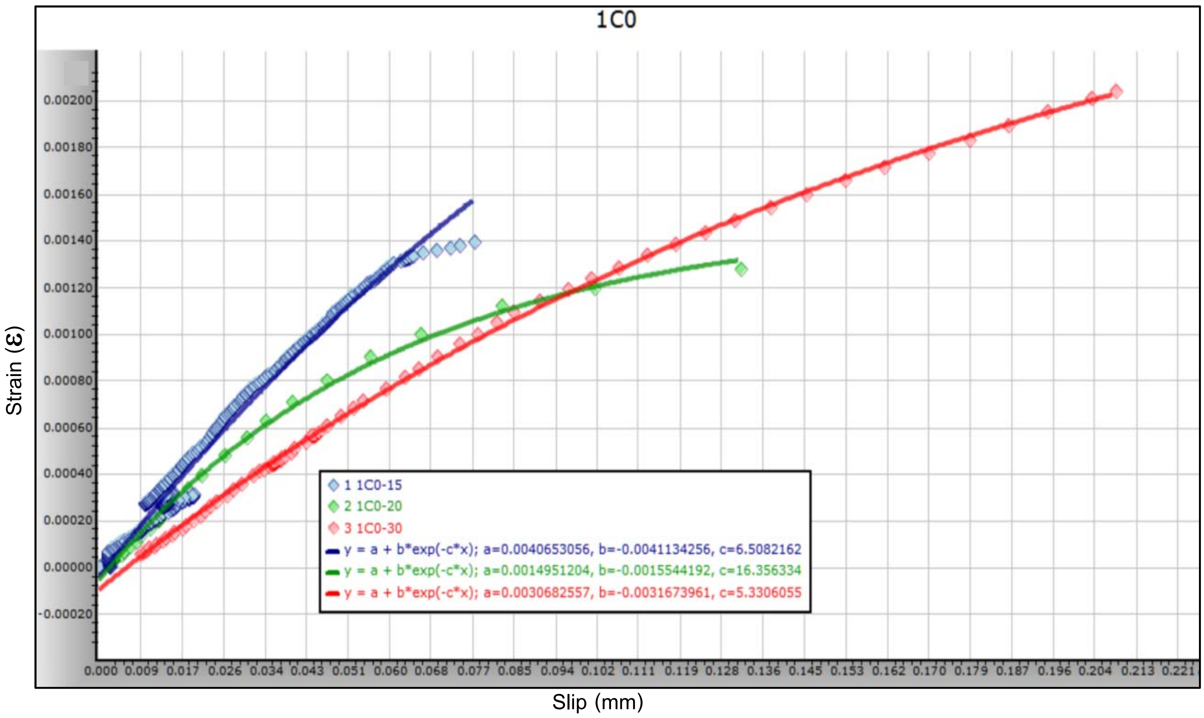

(a)

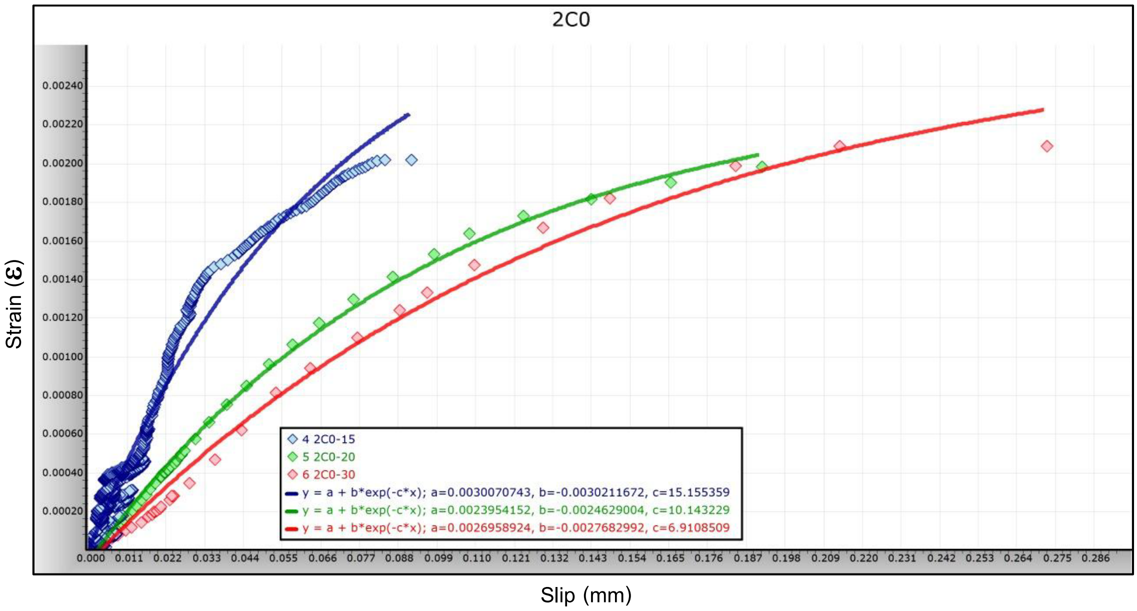

(b)

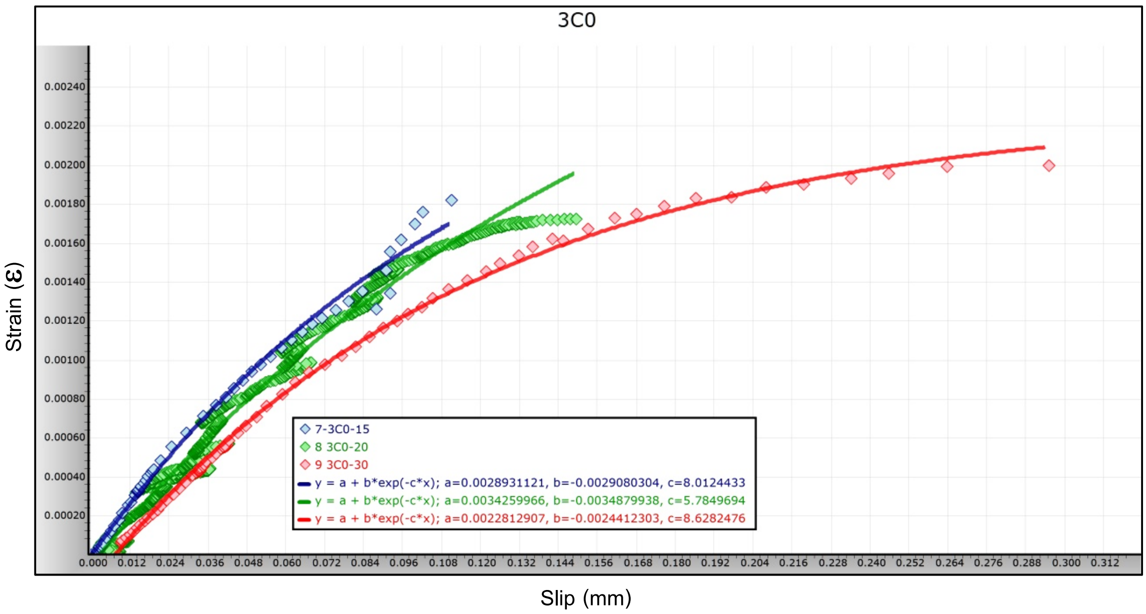

(c)

Figure43 Experimental and regression strain-slip relationship of 0 min. exposure time

From the equilibrium equation of Figure44,

$$\tau_i = E_f t_f \frac{d\varepsilon}{dx} = E_f t_f \frac{df(s)}{ds} f(s) \qquad (4.5)$$

So; $$\tau = A^2 B E_f t_f \, e^{-Bs}(1 - e^{-Bs}) \tag{4.6}$$

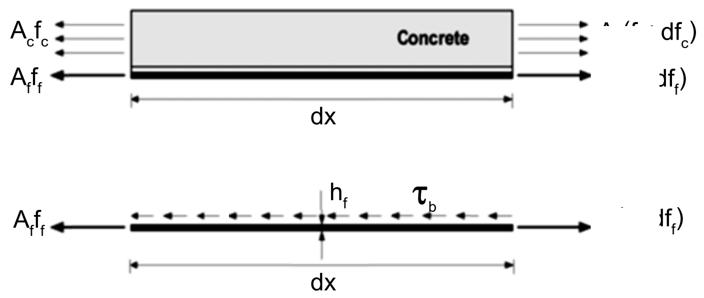

Figure 44 Free body diagram of single-lap pull out test

The interfacial fracture energy defined as

$$G_f = \int_0^{\infty} \tau \, ds = \frac{1}{2} A^2 E_f t_f$$

$$A = \sqrt{\frac{2G_f}{E_f t_f}} \tag{4.7}$$

Substituting equation 4.7 into equation 4.6 :

$$\tau = 2BG_f(e^{-Bs} - e^{-2Bs}) \tag{4.8}$$

However, difference points between Jianguo Dai et al's method and this experiment are diversity of concrete strength, concrete surface condition, variation of bond length and difference in bond testing which sould be comprised in this model espectially the effect of bond testing variation. From Figure44 shows the free body diagram of single-lap pull out method which is the Jianguo Dai et al's experiment. The shear stress-slip model in eqaution 4.6 are derived from the equiliribrium equation which all forces in this system are alined in horizontal direction. But in this research, the modified pull-out test are performed and has difference force aliements as shown in

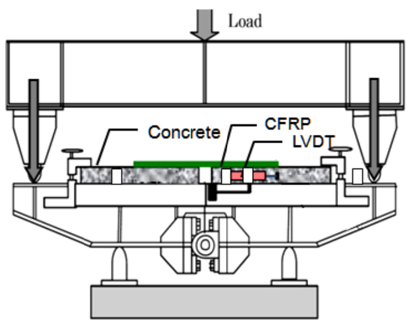

Figure46 Load direction of modified pull-out test

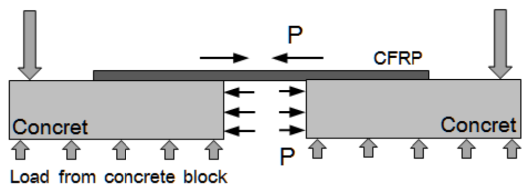

Figure45 Free body diagram of modified pull-out test

Figure46. Moreover, the shape of unbonded CFRP plate (between two concretes specimens) was bend as could be observed during testing because of load application in this experimental method. According from recent effects, the parameters ξ are suggested and applied in the shear stress-slip model for adjusting the effect of diversity of bond testing which equal to 1.95.

Therefore, the model of shear stress-slip relationship can be obtained from the modified pull-out test, which was expressed in equation 4.9 :

$$\tau = 2\xi B G_f \left(e^{-Bs} - e^{-2Bs}\right) \tag{4.9}$$

According from above equation, the parameters can be described as following:

τ = Shear stress or bond stress, MPa

G_f = Interfacial fracture energy, N/mm, (see equation 4.3)

B = Index of ductility of τ-s relationship which including the effect of FRP stiffness (kN/mm) and shear stiffness of adhesive (GPa/mm) as presented from Jianguo Dai et al.'s model.

$$B = 6.846(E_f t_f)^{0.108} \left(\frac{G_a}{t_a}\right)^{0.833}$$

From calculation, the parameter B in this research equal to 12.52 .

ξ = The adjusting parameter for considering the variation of bond testing which equal as 1.95.

From the comparisons between experimental and analytical of shear stress-slip relationship (see Figure48), the presented model can be shown the good agreement correspond to test results except the 30 cm of bond length specimens. The failure mode of those specimens was inaccurate which fail on 350 ksc compressive strength of concrete at ultimate tensile strength as reported in table 13. Therefore, in predicted relationship of 30 cm in bond length specimens shows obviously difference with the experimental results. However, when assess the suggested model with other experimental results from other researchers, the tendency quite conforms but some curves are difference which can be seen from maximum shear stress distinction due to variation of FRP's properties and test method as shown in Figure 47.

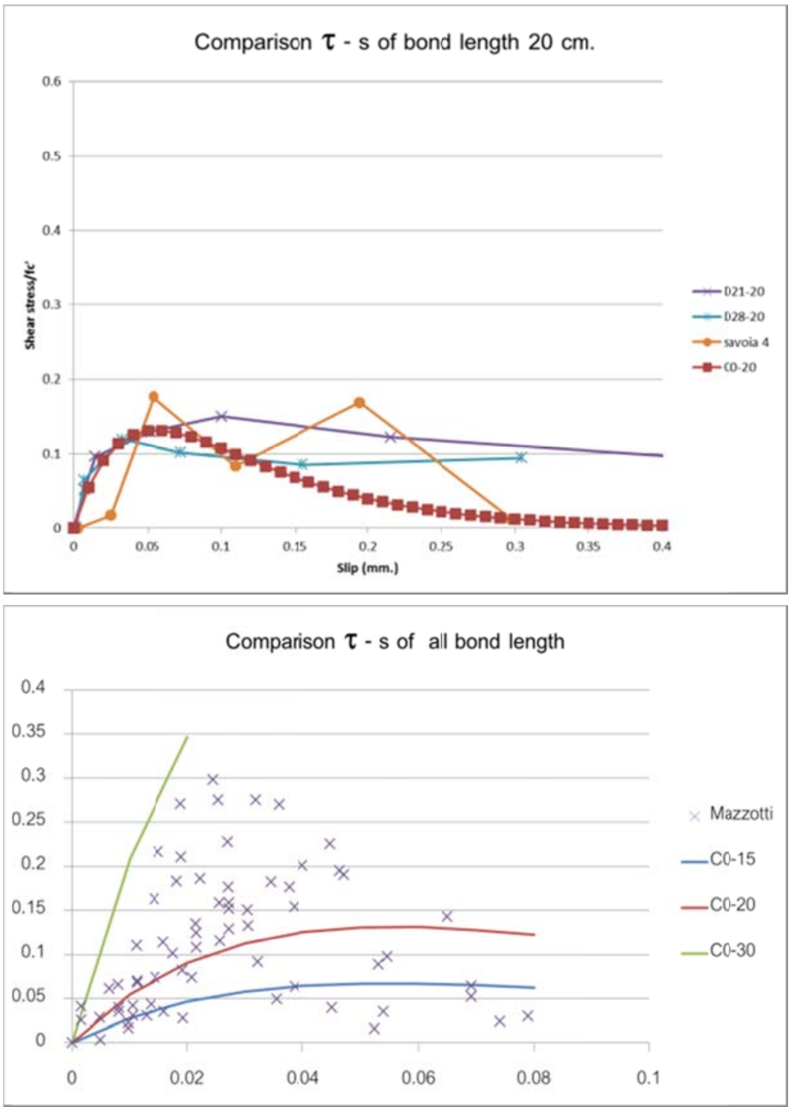

Figure47 Comparison between proposed model and previous test results from various studies

*Remark : Experimental datas in Figure47 reference from Donk-Suk Yang et al.[14], M. Savoia et al.[25], C.Mazzotti et al.[26]

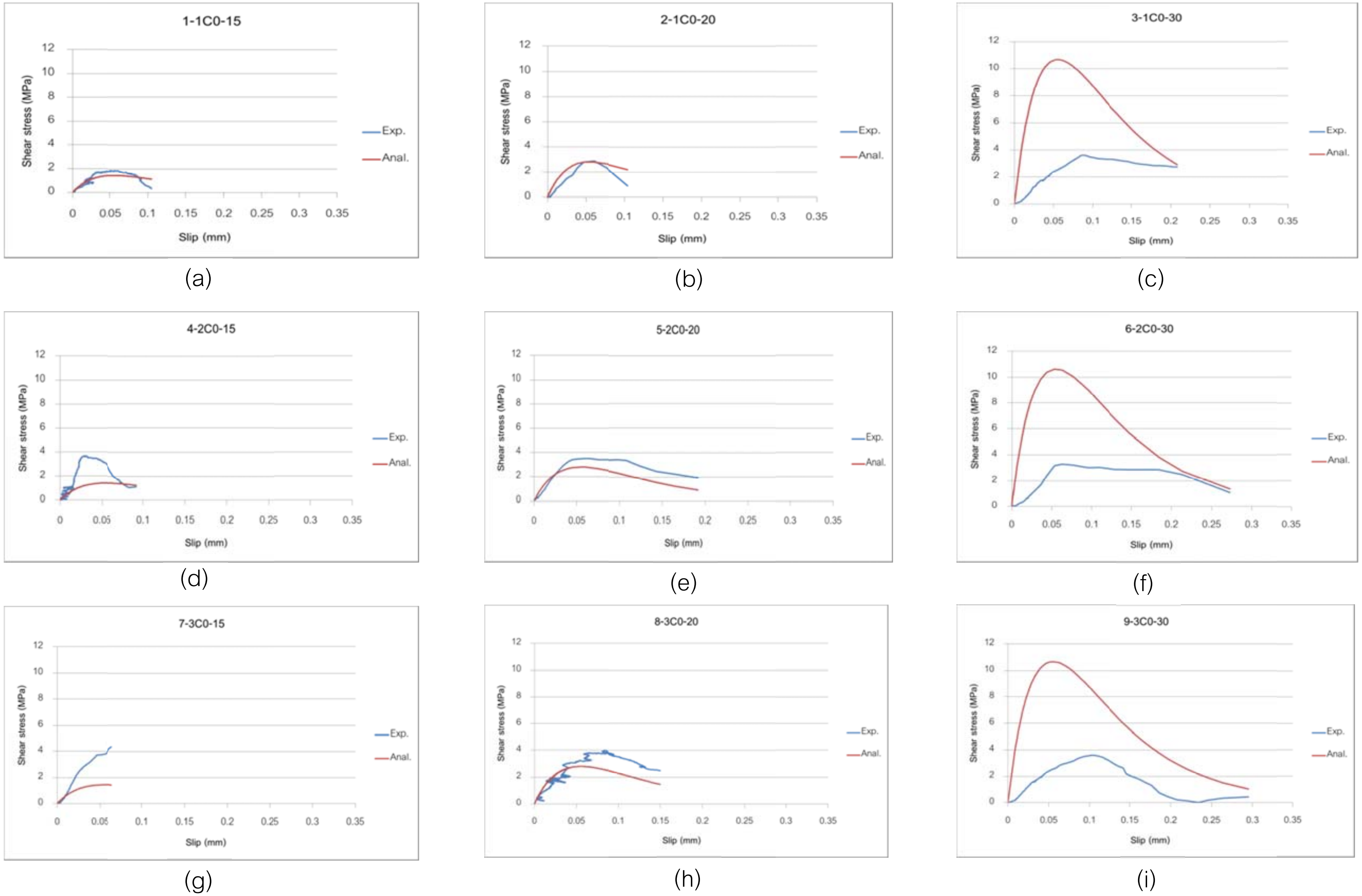

Figure48 Experimental and predicted shear stress-slip (τ-S) relationship of 0 min. exposure time

4.3.3 Relationship between shear stress-slip model of damaged concrete specimens (exposure time equal to 45 and 90 min.)

The formulation of shear stress-slip model in 45 min and 90min of exposure times can be conducted in the same as previous model which originated from the relationship of strain-slip at loaded end. However, from observation, the strain-slip relationship of both exposure times is difference from the non-fired concrete. Because the bonding between concrete and CFRP of the damaged specimens are destroyed from fire and leads to early debonding at the same bond length when comparing with the non-fired concrete series. Consequently, the slips of damaged concrete are shorter and provide the linear relationship between strain and slip instead of exponential function as shown in Figure 49.

The strain-slip relationship of damaged concrete series can be obtained from the modified pull-out test are expressed in equation 4.10.

$$\varepsilon = f(s) = As \tag{4.10}$$

Where, *A* is a regression constant between strain –slip curve.

From;

$$\frac{d\varepsilon}{dx} = \frac{df(s)}{ds}\frac{ds}{dx} = \frac{df(s)}{ds}\varepsilon = \frac{df(s)}{ds}f(s)$$

$$\tau = E_f t_f \frac{d\varepsilon}{dx} = E_f t_f \frac{df(s)}{ds} f(s)$$

Therefore,

$$\tau = E_f t_f A^2 s \tag{4.11}$$

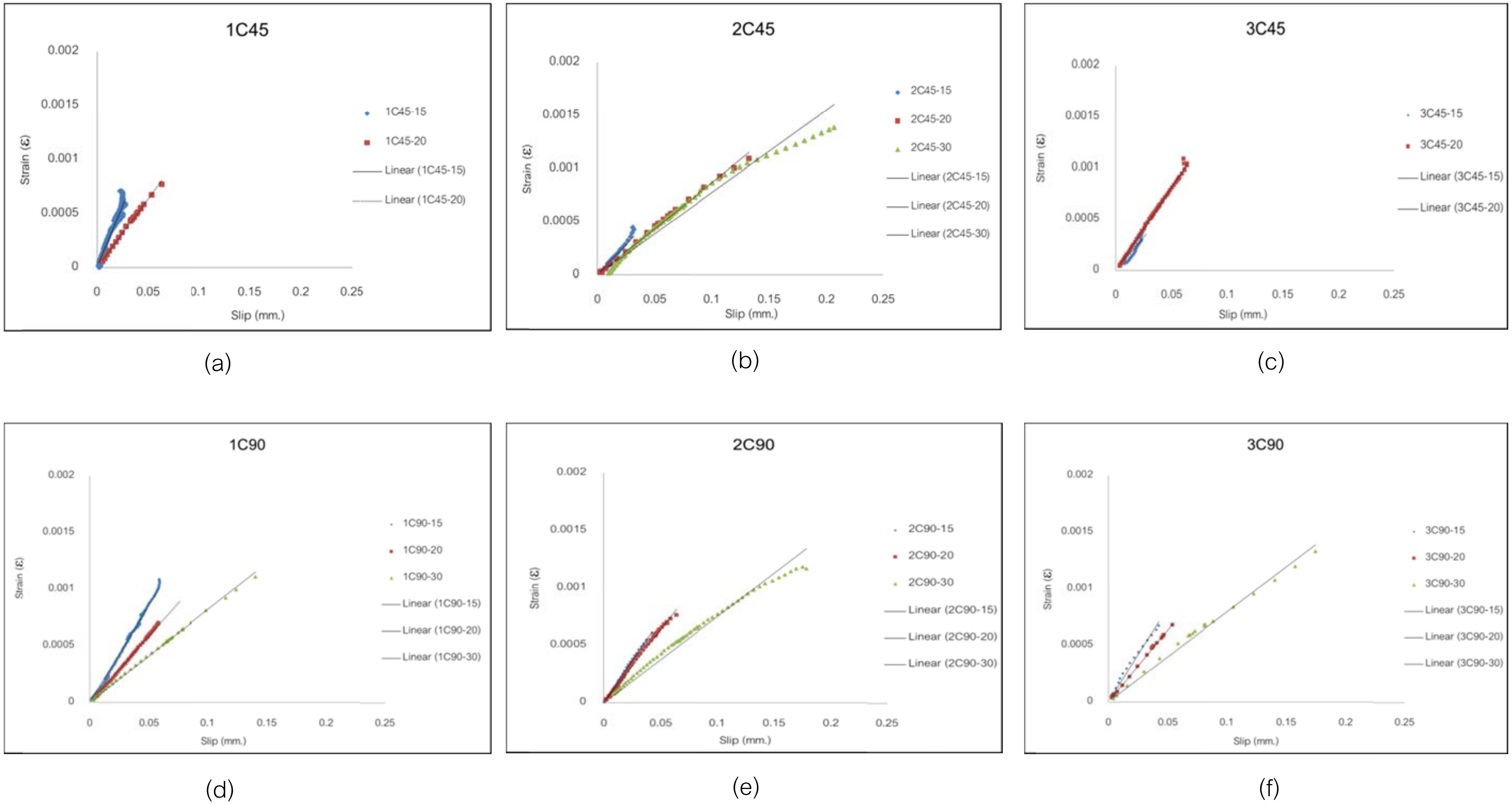

Figure49 The regressed strain-slip relationship of damaged concrete specimens

Table 14 Summary of regreassion parameters from strain and slip relationship

Specimens	*A*	*B*	R^2	Remarks
1C0-15	0.0041	6.5082	0.979	* Exponential regression $\varepsilon = f(s) = A(1-e^{-Bs})$
1C0-20	0.0015	16.3563	0.9968	
1C0-30	0.003	5.3306	0.9991	
2C0-15	0.0034	8.3322	0.9579	
2C0-20	0.0025	10.1432	0.9982	
2C0-30	0.0027	6.9109	0.9901	
3C0-15	0.0029	8.0124	0.9929	
3C0-20	0.0034	5.7850	0.9850	
3C0-30	0.0024	8.6282	0.9975	
1C45-15	0.0228	-	0.9442	* Linear regression $\varepsilon = f(s) = As$
1C45-20	0.0128	-	0.9961	
2C45-15	0.0115	-	0.9700	
2C45-20	0.0087	-	0.9970	
2C45-30	0.0078	-	0.9598	
3C45-15	0.0131	-	0.8204	
3C45-20	0.0163	-	0.9966	
1C90-15	0.0172	-	0.9951	
1C90-20	0.0118	-	0.9963	
1C90-30	0.0082	-	0.9985	
2C90-15	0.0146	-	0.9974	
2C90-20	0.0127	-	0.9962	
2C90-30	0.0075	-	0.9743	
3C90-15	0.0167	-	0.9848	
3C90-20	0.0127	-	0.9995	
3C90-30	0.0080	-	0.9883	

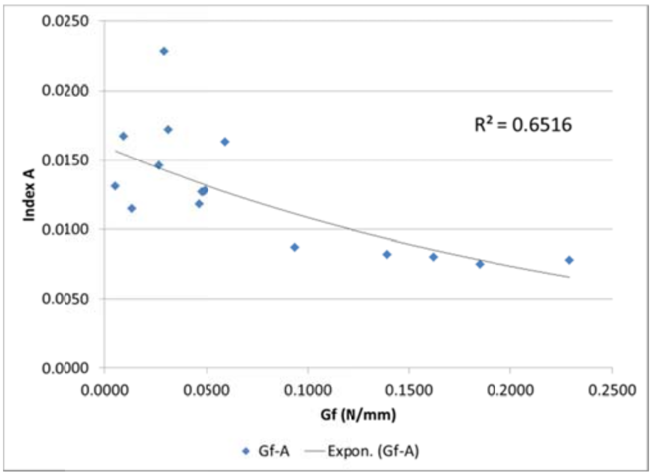

Figure50 The correlation of index A and G_f

According to equation 4.11, the parameter *A* can be defined and related to the interfacial fracture energy as performed in Figure50:

Therefore, the index *A* can be formulated as following expression:

$$A = 0.016e^{-3.872\,G_f} \tag{4.12}$$

Substituting equation 4.12 to 4.11,

$$\tau = 0.000256E_f t_f e^{-7.744\,G_f} s \tag{4.13}$$

Noted that, τ = Shear stress or bond stress, MPa

$E_f t_f$ = Stiffness of FRP, N/mm

G_f = Interfacial fracture energy, N/mm (see equation 4.3)

In fact, the bond behavior between CFRP and concrete after fire has not been studied from previous researcher. Therefore, the proposed model cannot compare and verify with other results. But the comparison in Figure 51 and 52 shows the good accession of predicted model correspond to experimental results. Accordingly, from the parameter ξ in shear stress-slip model of non-fired series which applies for adjusting the effect of different various conditions between Jianguo Dai et al's model and this research, it does not necessarily involve in bond-slip relationship of damaged series.

According to Figure 48, 51 and 52, the predicted models of shear stress-slip relationship which have been modified according to simple method as developed by Jianguo Dai et al. [15] can be properly corresponded to experimental results. In addition, the proposed model from this study can be appiled to numerical study for analyzing the effect of fire to damaged structure in further study.

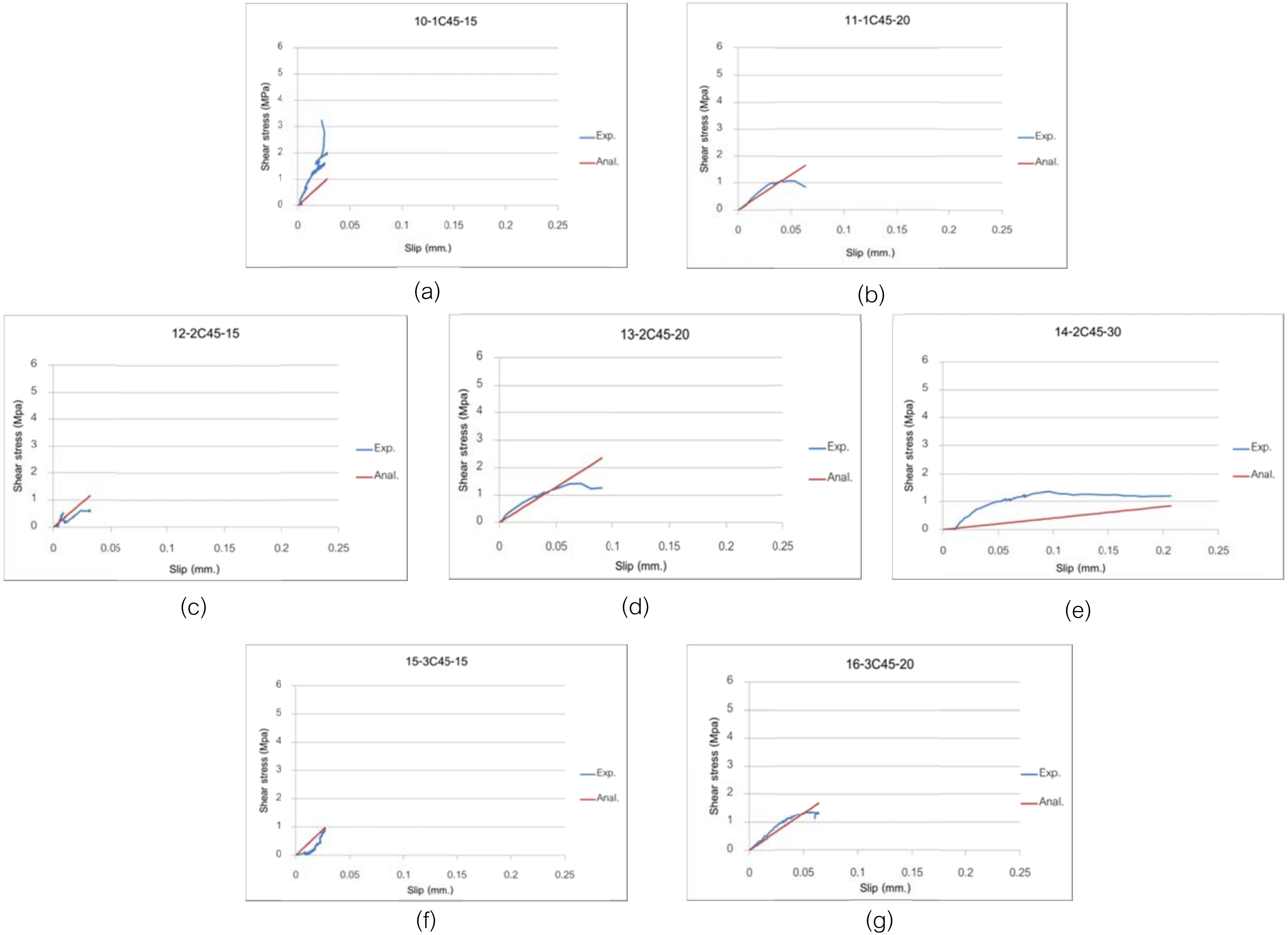

Figure51 Experimental and predicted shear stress-slip (τ-s) relationship of 45 min exposure time

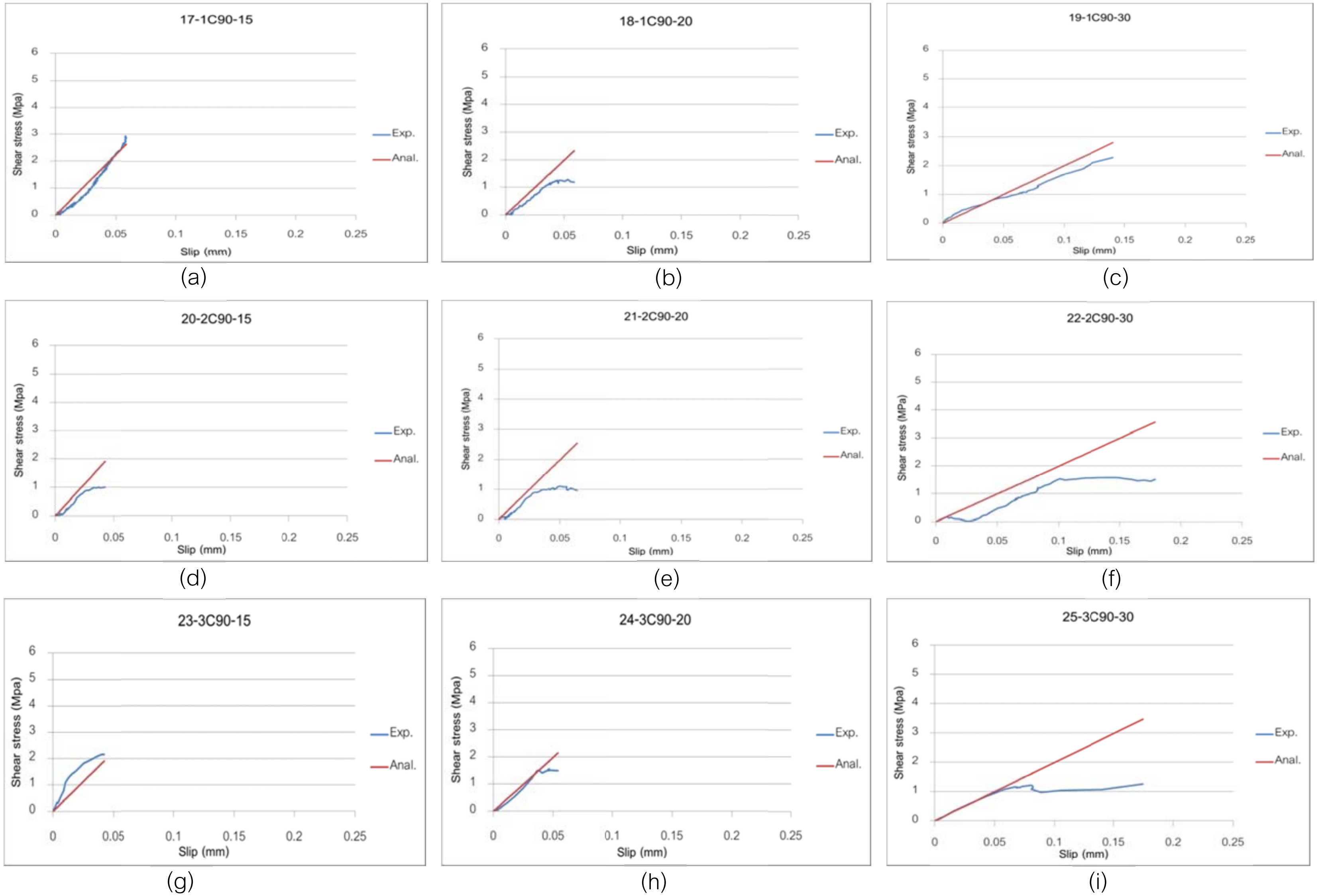

Figure52 Experimental and predicted shear stress-slip (τ-s) relationship of 90 min exposure time

CHAPTER V
CONCLUSIONS

5.1 Research summary

In this research, the modified pull-out test was performed to investigate bonding behavior of damaged concrete from fire with various parameters such as fired exposure time, bond length of CFRP plate and concrete covering. The research summary can be concluded corresponding to the objectives:

1. Damage from fire can create a large spalling on the concrete surface which has a direct effect on the bond between concrete and FRP. Consequently, the higher temperature can directly diminish the bond behavior between concrete and FRP as shown from various parameters such as surface tensile strength, interfacial bond strength, P_{max} and interfacial fracture energy, G_f which decreased according with increased in temperature.

2. The effect of fire can change the effective bond length. Because in the damaged concrete series, the increased bond length of CFRP can significantly increase the interfacial bond strength, P_{max} while the value of P_{max} of C0-20 and C0-30 series (normal concrete) are closer. Moreover, the effect of bond length has direct variation to the interfacial fracture energy, G_f, although the bond length will exceed the effective length because it can conduct more ductility instead of maximum tensile force.

3. The effect of concrete covering has been vanished with increasing of exposure time and it does not show the significantly effect on interfacial bond strength, P_{max} and interfacial fracture energy, G_f. Therefore, concrete covering has the least influent to bonding behavior between reinforced concrete after fire and CFRP plate.

4. The proposed shear stress-slip model are modified from Jianguo Dai et al.'s model [15] and show a good agreement between predicted and experimental results as shown in the discussion part. The proposed model includes the effect of all parameters as follows:

The model of interfacial fracture energy including the effect of various parameters :

$$G_f = 0.0157\, e^{0.0134BL-0.022T} \tag{5.1}$$

Where, G_f = Interfacial fracture energy, N/mm

BL = Bond length of CFRP plate, mm.

T = Exposure time, min.

In nonfired concrete series, the shear stress-slip relationship can be proposed as:

$$\tau = 2\xi B G_f (e^{-Bs} - e^{-2Bs}) \tag{5.2}$$

Where, τ = Shear stress or bond stress, MPa

G_f = Interfacial fracture energy, N/mm, (see equation 5.1)

B = Index of ductility of τ-s relationship which including the effect of FRP stiffness and shear stiffness of adhesive as presented from Jianguo Dai et al.'s model. In this research, the parameter B equals to 12.52.

ξ = The adjusting parameter for considering diversity of bond testing which equal as 1.95.

On the other hand, in damaged concrete series which were fired at difference exposure times (45 and 90 min.), the shear stress-slip model can be proposed as:

$$\tau = 0.000256 E_f t_f e^{-7.744\, G_f s} \tag{5.3}$$

Where, τ = Shear stress or bond stress, MPa

$E_f t_f$ = Stiffness of FRP, N/mm

G_f = Interfacial fracture energy, N/mm (see eq. (5.1))

5.2 Suggestions for further study

1. In the bond test procedure, failure mode is one of the factors that affects the accuracy of bonding behavior. Therefore, the FRP designing and installation are very important as it has a great influence on the occurred failure mode. In this study, some specimens did not fail with debonding at concrete substrate which referred to imprecise empirical model.

2. For greater accuracy of shear stress-slip model, the number of fired specimens should be increased with increasing bond length simultaneously due to studying effect of fire to effective bond length and improving accuracy of empirical model.

3. The proposed shear stress-slip model is formulated from experimental data, thus, for further improvement on its accuracy, application on numerical study is needed. In addition, this proposed model can be applied to finite element analysis for analyzing bonding behavior and failure characteristic of damaged structure under low fire severity.

4. Refer to Thailand regulation, every structures should be resisted the damage from fire at least 3 hours. But according to the research summary, the effect of fire can extremely destroy the bonding behavior of concrete and CFRP even though in lower level of fire such as 45 min. Therefore, repairing of concrete surface before attach FRP

should be considered which refer to concern about the influence of repairing material to FRP in further study.

REFERENCES

[1] Teng, J. G., et al, FRP Strengthened RC Structures, England:John Wiley & Sons, Ltd, 2002.

[2] ACI Committee 440, Guide for the Design and Construction of Externally Bonded FRP Systems for Strengthening Concrete Structures, ACI 440.2R-02, American Concrete Institute, Farmington Hills, Michigan, July 2002.

[3] Hiroyuki, Y., Wu, Z., Analysis of Debonding Fracture Properties of CFS Strengthened Member Subject to Tension, Non-metallic (FRP) Reinforcement for Concrete Structure, Proceedings of the Third International Symposium, Sapporo, 1997, 287-294.

[4] Tanaka,T. Shear Resisting Mechanism of Reinforced Concrete Beam with CFS as Shear Reinforcement, Graduation Thesis, Hokkaido University, 1996.

[5] Meada et al., A Study on Bond Mechanism of Carbon Fiber Sheet, Non-metallic (FRP) Reinforcement for Concrete Structure, Proceedings of the Third International Symposium, 1997, 279-285.

[6] Holzenkämpfer, O., Ingenieurmodelle des Verbundes geklebter Bewehrung für Betonbauteile, Doctoral dissertation, TU Braunschweig, 1994.

[7] Täljsten, Plate Bonding Strengthening of Existing Concrete Structure with Epoxy Bonded Plates of Steel or Fibre Reinforced Plastic, Doctoral dissertation, Luleå University of Technology, 1994.

[8] Yuan, H., Wu, Z., Interfacial Fracture Theory in Structures Strengthened with Composite of Continuous Fiber, Proceeding of Symposium of China and Japan, Science and Technology of 21^{st} Century, 1999, 142-155.

[9] Yuan, H., Wu, Z.S. and Yoshizawa, H., Theory Solutions on Interfacial Stress Transfer of Externally Bonded Steel/composite Laminates, Journal of Structural Mechanics and Earthquake Engineering, JSCE, No.675/1-55, 2001, 27-39.

[10] Neubauer, U., Rostásy, F.S., Design Aspects of Concrete Structures Strengthened with Externally Bonded CFRP Plates, Proceedings of the Seventh International

Conference on Structural Faults and Repairs, edited by M.C. Forde, Engineering Technics Press, Edinburgh, UK, 1997, 109-118.

[11] van Gemert, D., Force Transfer in Epoxy-bonded Steel-concrete Joints, International Journal of Adhesion and Adhesives, No.1, 1980, 67-72.

[12] Chaallal, O., Nollet, M. J., Perraton, D., Strengthening of Reinforced Concrete Beams with Externally Bonded Fibre-reinforced-plastic Plates: Design Guidelines for Shear and Flexure, Canadian Journal of Civil Engineering, Vol. 25, No. 4, 1998, 692-704.

[13] Khalifa, A., Gold, W. J., Nanni, A., Aziz, A., Contribution of Externally Bonded FRP to Shear Capacity of RC Flexural Members, Journal of Composites for Construction, ASCE, Vol. 2, No. 4, 1998, 195-203.

[14] Dong-Suk Yang, Sung-Nam Hong and Sun-kyu Park, Eperimental Observation on Bond-Slip Behavior between Concrete and CFRP Plate, International Journal of Concrete Structure and Materials, Vol.1, No.1, December 2007, 37-43.

[15] Dai, J.G., et al., Development of the Nonlinear Bond Stress-Slip Model of Fiber Reinforced Plastics Sheet-Concrete Interfaces with a Simple Method, Journal of Composites for Construction, ASCE, Vol.9, No.1, February 1, 2005, 52-62.

[16] Ingberg, S.H., et al., Combustible Content in Buildings. (BMS 149). Washington, D.C. :National Bureau of Standard, 195.

[17] ASTM DESIGNATION : E119-98: Standard Test Methods for Fire tests of Building Construction and Materials,

[18] Omer Arioz., Effects of Elevated Temperature on Properties of Concrete., Fire Safety Journal, 2007, 516-522.

[19] Lin., T.D., et al., Flexure and Shear Behavior of Concrete Beams during Fires., ACSE : Journal of Structural Division 117, February 1991, 440-458.

[20] Songkiat Hansanti, Behaviors of reinforced concrete beams after fire, Master Thesis, Department of Civil Engineering, Chulalongkorn University, 2001.

[21] ASTM International, 2008 Annual Book ASTM Standards Section4 Construction.,vol. 04.02, Concrete and Aggregates, 2008.

[22] The International Federation for Structural Concrete (fib) as Bulletin 14, Externally bonded FRP reinforcement for RC structures, Technical report on the design and use of externally bonded fibre reinforced polymer reinforcement (FRP EBR) for reinforced concrete structures, Bulletin 14,July, 2001.

[23] Kobayashi, A., Matsui, S., Kishimoto, M., Fatigue Bond of Carbon Fiber Sheets and Concrete in RC Slabs Strengthened by CFRP, Proceedings of FRPRCS-6 (Edited by Tan, K. H.), Vol.2, 865-874, 2003.

[24] Chen, J.F., Teng, J.G. Anchorage Strength Model for FRP and Steel Plates Attached to Concrete, Journal of Structural Engineering, ASCE, Vol.127, No.7, 2001,784-791.

[25] Savoia, M., et al., Non Linear Bond-Slip Law for FRP-Concrete Interface, Fibre-reinforced polymer reinforcement for concrete structures : proceedings of the Sixth International Symposium on FRP Reinforcement for Concrete Structures (FRPRCS-6), July, 2003, 163-167.

[26] Mazzotti, C, Ferracuti, B. and Savoia, M., 2005, FRP - concrete delamination results adopting different experimental pure shear setups, International Conference on Fracture: Proceedings of ICF XI, March, 2005.

BIOGRAPHY

Miss Pornpen Limpaninlachat graduated her Bachelor Engineering degree in Civil Engineering from Chulalongkorn University in 2009. According from her fondness, she would like to obtain the advanced knowledge of structural engineering. She continued her Master's degree in structural civil engineering at Chulalongkorn University in the same year under the guidance of Assistant Professor Dr. Withit Pansuk. For two years and a half of studying in Master's degree, she had studied new interesting knowledge of advanced concrete structure and decided to do her research on this kind of field. She successfully graduated the requirements for the Master of Engineering degree in 2012.